Geomorphology of Dune Blowouts, Cape Cod National Seashore, MA

by

Alexander B. Smith

August, 2013

Director of Thesis: Paul Gares

Major Department: Geography

Dune blowouts are common erosional features that develop in dune fields worldwide. At Provincelands dunes in Cape Cod National Seashore, blowouts are eroding into shore parallel transverse dunes and the trailing arms of inland parabolic dunes. High spatial and temporal resolution data was collected with Terrestrial Laser Scanning. This allows for the detailed topographic mapping of blowouts that are monitored through time. Large scale geomorphic changes are driven by high magnitude northerly storm events that occur in the fall and winter seasons. Storm events from various incident angles are being topographically steered into the blowout and areas with increased gradient of slope within the blowouts are eroding more rapidly. Incipient embryo blowouts are developing in the lee of elevated dune crests and potentially become captured through the coalescence of landforms. This embryo capture leads to rapid modifications to the host landform and provides new considerations for the larger blowout evolutionary model. Blowouts are ubiquitous features at Cape Cod National Seashore making this an ideal study and the ability to collect high resolution geomorphic data that has greatly increased our knowledge on blowout evolution.

Geomorphology of Dune Blowouts, Cape Cod National Seashore, MA

A Thesis

Presented To the Faculty of the Department of Geography

East Carolina University

In Partial Fulfillment of the Requirements for the Degree

Masters of Arts

by

Alexander B. Smith

August, 2013

Geomorphology of Dune Blowouts, Cape Cod National Seashore, MA

by

Alexander B. Smith

APPROVED BY:

DIRECTOR OF
DISSERTATION/THESIS: _____
(Paul Gares, PhD)

COMMITTEE MEMBER: _____
(Thad Wasklewicz, PhD)

COMMITTEE MEMBER: _____
(Scott Lecce, PhD)

CHAIR OF THE DEPARTMENT
OF GEOGRAPHY:_____
(Burrell Montz, PhD)

DEAN OF THE
GRADUATE SCHOOL:_____
Paul J. Gemperline, PhD

ACKNOWLEDGEMENTS

I would like to thank NSF for funding the research project 'Blowout Dynamics at Cape Cod.' I would also like to thank East Carolina University and Louisiana State University for additional funding for continued research at Cape Cod National Seashore, MA. I would like to thank professors Paul Gares, Thad Wasklewicz, Patrick Hesp, Ian Walker, and Scott Lecce for providing guidance throughout my research efforts. Special thanks to Kathryn Reavis, Kimia Abhar, and Kailey Adams for assisting with data collection in the field. Finally, I would like to acknowledge the Department of Geography at East Carolina University for providing an excellent environment for learning and continual growth as a student.

TABLE OF CONTENTS

LIST OF TABLES

LIST OF FIGURES

CHAPTER 1: INTRODUCTION

Blowouts are common erosional features that develop in dune landscapes where there is high energy and abundant sediment supply (Hesp, 2002). Blowouts are initiated largely due to topographic disturbances in dune structures or by the removal of vegetation, both of which leave dunes vulnerable to continual aeolian erosion and blowout development (Hesp and Hyde, 1996; Hesp, 2002). Saucer and trough shaped blowouts are the most common forms of development. Regardless of shape, certain sub-landform features are shared between both blowout shapes including deflationary floor, lateral wall, and depositional lobes (Hesp, 2002). Blowouts have a unique process-form relationship between airflow and topography. Topographic steering and acceleration of air flow magnifies the erosion occurring within blowouts. The larger geomorphic significance of blowouts is in their ability to rapidly deflate in the area of initiation and transfer large amounts of sediment to depositional lobes and back dune deposits (Gares and Nordstron, 1996; Hesp, 2002; and Anderson and Walker, 2006).

Blowouts have the ability to mobilize large amounts of sediment within dune-fields. A number of studies have provided the basis of our knowledge on the geomorphology of blowouts (Jungerius and van der Muelen, 1989; Gares, 1992; Gares and Nordstrom, 1995; Hugenholtz and Wolfe, 2006; and Kayhko, 2007), but they all have limitations in the spatial and temporal resolution at which these studies were conducted. Advances in technology (e.g. Terrestrial Laser Scanning) have led to an increased ability gather high-resolution spatial and temporal data. These advances in data collection provide the potential to increase our knowledge of dune blowout dynamics through innovative geomorphic measurements that allow for the creation of detailed sediment budgets and rim morphometrics. Herein, I have developed two studies that leverage high-resolution spatial and temporal data to provide a detailed assessment of the geomorphic

evolution of dune blowouts. More specifically, the results presented in two separate research papers (i.e. Chapters 2 and 3), detail dune blowout evolution at multi-temporal scales (i.e. annual and seasonal) and at different spatial scales (i.e. landform and sub-landform).

Geomorphic Setting

This study is conducted at Cape Cod National Seashore where there are a high number of blowouts at varying stages of evolution. The large numbers of dune blowouts are in part a response to the optimal conditions for development (i.e. high energy and large sediment supply). Beach parallel dune ridges are exposed to high magnitude storm events that occur predominantly in the winter (Fig. 2). This has led to the prevalence of blowouts in this dune system, providing a perfect location in which to study the evolution of these landforms at multiple stages of development. Large well developed blowouts have left an indelible impact on the larger landscape, while incipient blowouts are just beginning their role as areas of rapid deflation. Embryo blowouts, or incipient blowouts forming downwind of the crest of larger blowouts or ridges, are a unique type of blowout that has been identified at this study site. The significance of these features lies in their ability to expand rapidly and eventually to lead to the breach of the crest separating the embryo from its host. These features appear to have significant impact on the geomorphology of the host blowout following embryo dune capture. Well developed and incipient embryo blowouts will be studied in detail to provide a better understanding of their role within the landscape and their contribution to the larger blowout evolutionary model.

Figure 1: The Northern extent of Cape Cod National Seashore. Shore parallel dunes are exposed to high magnitude landward storm events that occur in the fall and winter months.

The results of the research projects will be presented as two independent research articles (i.e. Chapters 2 and 3). Each of which will have its own literature review, study site, methodology, results, discussion, and conclusion. These chapters are designed to be ready for publication and both will contribute to the larger blowout geomorphology literature. The final chapter will be a conclusion that will integrate the major findings of both articles into one cohesive summary. Since the chapters are independent of one another they will address different core research questions. Research questions 1-3 will be addressed in the Chapter two (i.e. Annual and Seasonal Geomorphology of a Trough Blowout, Cape Cod National Seashore, MA) and research questions 4-5 will be addressed in Chapter three (i.e. Geomorphic Impact on the Development and Capture of Embryo Dune Blowouts, Cape Cod National Seashore, MA).

Research Questions

1. What geomorphic changes occur within the blowout and across the depositional lobe during varying temporal scales? What do these temporal scales (i.e. annual and seasonal) indicate about the geomorphic evolution of the study site?
2. How will the classification of sub-landform features provide insight to larger scale trends occurring within the blowout? Will slope and curvature allow for the classification of geomorphic zones and can these zones be clearly delineated?
3. Can regional wind data be used to highlight localized topographic steering within blowouts? What inferences can be made by analyzing the relationship of regional wind patterns to on-site sediment drift?
4. What impact does the development and eventual capture of embryonic dunes have on the continual geomorphic evolution of the adjacent blowout or dune ridge? Can we determine where and how rapidly these features are evolving?
5. How does our knowledge of embryos lead to the consideration of a new theoretical model that explains the initiation and expansion of these features? What is the applicability of this model at various locations?

Chapter 2: Annual and Seasonal Geomorphology of a Trough Blowout, Cape Cod National Seashore, USA

Introduction

Dune blowouts are common erosional features that develop in aeolian landscapes and act as conduits allowing for the transfer of large amounts of sediment to depositional lobes and backshore dune deposits (Gares and Nordstrom, 1995; Hesp, 2002; and Anderson and Walker 2006). Blowouts initiate in otherwise stable areas by wave and aeolian processes, climate change, loss of vegetation, or anthropogenic disturbances (Hesp and Hyde, 1996; Hesp, 2002; and Hesp and Walker, 2012). After initiation, incipient blowouts experience negative erosional feedback from aeolian processes which continually work to expand these features (Hugenholtz and Wolfe, 2006). As dune blowouts develop into saucer or trough shapes, the topography greatly modifies the boundary layer conditions affecting velocity and directionality of airflow (Hesp, 2002). These unique process form relationship between blowouts and the acceleration and steering of airflow has been the primary focus of many studies focusing on dune blowouts. Relatively few in depth studies focusing on the geomorphology of dune blowouts have been conducted (Jungerius and van der Meulen, 1989; Hugenholtz and Wolfe, 2006; and Kayhko, 2007). These geomorphic studies have focused primarily on long-term decadal changes in blowouts; however, there is a need to understand changes taking place at the annual and seasonal scale in order to capture rapid geomorphic modifications to these landforms.

Geomorphology

Dune Blowouts tend to form in high energy environments with large sediment supplies and are common in both coastal and continental dune fields (Hesp, 2002). Blowouts evolve into

two primary forms; deep elongated troughs and shallow semi-circular saucer shapes (Hesp, 2002). There are also common sub-landform features identified in field observations, including the deflation basin or floor, lateral slope or wall, transportation ramp, scarp, and throat. While previous sub-landform observations have been largely empirical there is thought to be a relationship between slope and the morphodynamics of dune blowouts. Hugenholtz and Wolfe (2006) found that erosion pins that were located in areas of elevated slope experienced rapid topographic deflation. Elevated slopes within blowouts are believed to be most active and are commonly found to experience grain avalanching and slump failure leading to increased erosion in these areas.

Previous geomorphic studies have largely utilized erosional pins to study surface elevation changes by placing pins in transects across the surface of the blowout and depositional lobe (Gares, 1992; Gares and Nordstrom, 1995, and Hansen et al, 2009), grids across the surface (Pluis, 1992; Hugenholtz and Wolfe, 2006), and at locations around the rim (Jungerius & van der Meulen, 1989). Also Tachymetric leveling has been used to measure elevation changes within blowouts using stake transects as reference points (Kayhko, 2007). These techniques can provide highly accurate measurements of erosion and accretion but problems exist when interpolating the results into iso lines or grids in which elevation changes and volume can be estimated. Limitations in spatial the resolution of these studies have allowed for ambiguity to exist in peripheral areas of the landform.

Process Form Relationship

Blowouts have unique process-form relationships where the local topographic characteristics of these features are inextricably linked to steering and acceleration of airflow and

consequently to the continued evolution of the landform. The primary axis of blowouts tend to be oriented in the direction of incoming high magnitude winds (Gares and Nordstrom, 1995). Trough blowouts tend to steer incoming wind directions parallel to their primary axis (Hesp and Hyde 1996, Hesp and Pringle, 2001; and Hansen et al, 2009), but both trough and bowl blowouts have been observed to have zones of recirculation of airflow of up to 180° off of the incoming wind direction (Fraser et al, 1998; and Hugenholtz and Wolfe, 2009). Localized non-logarithmic jets have been recorded in both trough and saucer blowouts as airflow become compressed and accelerated because of unique boundary layer conditions (Hesp and Hyde 1996; Hugenholtz and Wolfe, 2009; and Hesp and Walker, 2012). Airflow has also been shown to decelerate as it enters the blowout and on the lee of the crest on the depositional lobes as airflow expands in localized flow separation zones (Gares and Nordstrom, 1995; Hesp and Hyde, 1996; Hugenholtz and Wolfe, 2009; Hesp and Walker, 2012). As airflow moves up the axis, wind becomes compressed and reaches its highest speeds at the crest of the blowout rim (Hesp and Hyde, 1996).

Variations in boundary layer steering and acceleration of airflow can lead to asymmetrical development of blowouts (Gares and Nordstrom, 1995). Studies have also shown a more linear trend of blowout evolution as incoming winds are steered parallel to the axis (Hesp and Pringle, 2001; and Hansen et al, 2009). The size of a dune blowout can be a limiting factor when it becomes too deep or wide to promote continued erosion as the ability of these features to produce jet flows becomes reduced (Gares and Nordstrom, 1995; Hesp, 2002). Other factors that have an impact on the size of blowouts include the competence of winds to transport sediment, internal sediment supply of the blowout, and erosion down to the water table that inhibits continual transport (Hesp and Walker, 2012; Hugenholtz and Wolfe, 2006). Gares and Nordstrom (1995) proposed a cyclical model of blowout evolution, which includes initiation,

expansion, and eventual stabilization of blowout dunes following a critical threshold being reached. Others have observed a transition from large blowouts, especially trough blowouts, to small parabolic dunes in which the critical size of the blowout was never fully reached because of abundant sediment supply and high magnitude winds (Hugenholtz and Wolfe, 2006; Hansen et al., 2009).

Seasonality

There are several seasonal variations that play a role in sediment transport among blowout features. One of the most significant seasonal variations is the role of vegetation which Gares and Nordstrom (1995) describe as being the critical determinant for potential deflation of foredune structures, which is a precursor for incipient blowout development. Vegetation stabilizes the foredune and other dune structures making it resistant to erosion and possible blowout initiation (Hesp 2002). On the surface of the blowout a microbial crust in the form of algae temporarily stabilizes sections of larger blowouts in the summer months (Pluis, 1991). In winter months, when flora tends to die off or become buried, there is a greater potential for aeolian processes to transport large quantities of sediment through the blowout because of a loss of stability within the preexisting structures due to vegetation loss (Davidson-Arnott and Law 1990). While this potential is greatest in the winter months, other factors may affect the actual transport including high moisture content of the sediment, snow cover, or frozen ground (Davidson-Arnott and Law, 1990). Surface moisture is particularly important at controlling sediment transport throughout the year because small increases in moisture content (4-6%) require an increase in wind speed of 8-10% to transport the dampened sediment (Davidson-Arnott et al., 2007). Sediment that is saturated is greatly resistant to aeolian processes and can only be transported through high magnitude events. Soil moisture content can vary greatly at the

time scales ranging from days to seasons due to differences in solar aspect, length of days (Hugenholtz and Wolfe, 2006), and evaporation (Davidson-Arnott et al., 2007). Thus, an increase of aridity of the sediment would be expected in summer when the sun is at its highest angle in the sky, the days are long, and temperatures are high, all leading to increased evaporation potential.

Based on these factors, summer would seem to be a critical period for blowout initiation and development (Hesp 2002). However, these seasonal variations are misleading because the high wind speed events that produce erosion and deposition more commonly occur from late fall to early spring. The geomorphic responses of blowout features are greatly linked to storm events which may not correspond to expected trends accounting for seasonal variables (Hesp and Walker, 2012). Optimal sediment transport conditions result from the combination of low vegetation cover, low moisture content and high wind speed events. This suggests that the ideal period for landscape change associated with aeolian processes would occur in the fall or spring when temperatures are high enough to produce evaporation, which keeps the surface sediment relatively dry, vegetation density is low at the onset of winter or just beginning to thicken at the end of winter, and wind events are sufficiently powerful to move sand.

Objectives

The focus of this study is to provide an in depth geomorphic analysis of topographic changes occurring on the annual and seasonal temporal scales. High spatial and temporal resolution will be achieved through repeat topographic surveys and will be able to accurately quantify both large and small scale changes. This will provide a greater understanding of the geomorphology of blowouts by providing detailed morphometry and sediment budget

measurements on a multi-temporal scale. Geomorphic zones within the blowout will be classified and quantified based on volumetric changes. This will provide a sub-landform scale that will compliment the global changes by providing insight into how zones within the larger scale feature impact larger trends of geomorphic change. Lastly the regional wind regime will be studied based on the potential for sediment transport. While it has been well documented that local topography modifies boundary layer flow, the regional context will provide an understanding of the impact of wind events in relation to sediment drift within a blowout

Study Site

The study site is located at Provincelands Dunes, part of the Cape Cod National Seashore on the Northern end of Cape Cod (Fig. 1). Provincelands Dunes consist of a sizeable Holocene parabolic dune complex containing eleven large discrete parabolic dunes inland and a transverse dune system seaward along the beach (Forman et al, 2008). Blowouts at Provincelands Dunes have developed along the inner transverse dune ridges and on the trailing arms of the parabolic dunes both of which face northwest to northeast toward the beach. Blowout initiation generally occurs on the elevated dune crests on the seaward side of the ridges, which are exposed to strong northerly winds that are typical of the winter months. European settlement and the associated deforestation in this region may have reactivated the dune complex near the end of the 17th century (Forman et al., 2008). The removal of the forest cover has provided a large amount of available sediment for reactivation by aeolian forces which have lead to the continuous evolution of the landscape over the past three centuries.

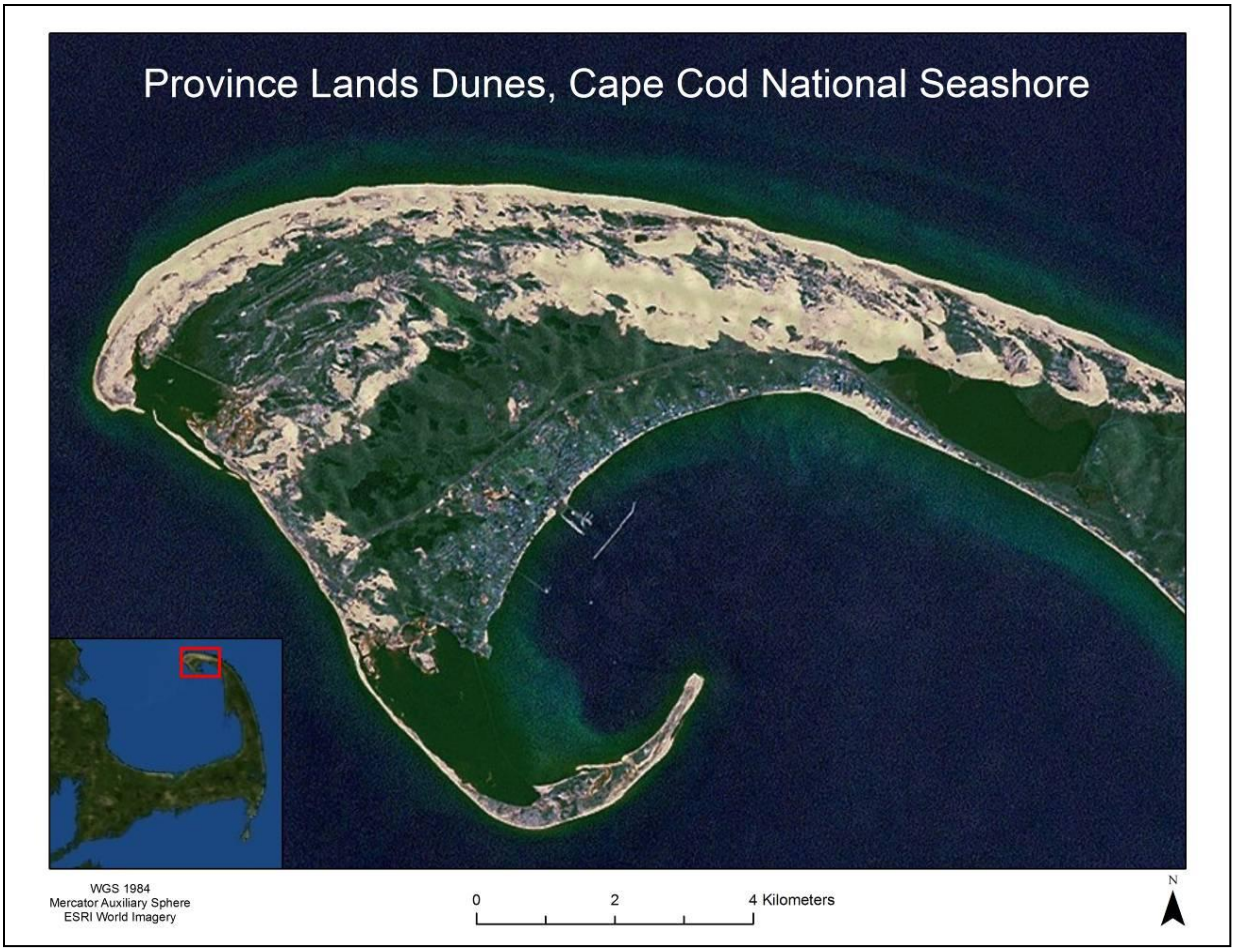

Figure 2: Province Lands Dunes is a Holocene dune complex in the Cape Cod National Seashore which has a high density of blowout dunes due to the high-energy environment and available sediment supply.

A large trough blowout (42°04'46.35"N, 70°12'29.31"W) was selected for this study. The blowout has eroded into the side of an interior dune ridge that is located roughly three hundred meters inland from the coast. The axis extends from the throat to the rim crest at approximately 292.5 degrees, and is primarily exposed to winds coming from the northwest. The active surface of the blowout is mostly free of vegetation while the depositional lobe has dense vegetation mainly consisting of American Beach Grass *(Ammophila brevilgulata).* Several other floral

species also grow on the depositional lobe including poison ivy *(toxicodendron radicans)*, as well as woody shrubs and bushes including Northern Bayberry *(Morella pensylvanica)*, Beach Heather *(Hudsonia tomentosa)*, and Beach Plum *(Prunis maritime)*. The American Beach grass often loses vitality or becomes buried during the winter months while the woody species become islands, resistant to erosion of the depositional lobe year round.

Methodology

Data Collection

The geomorphic change detection is accomplished on the blowout with the aid of repeat Terrestrial Laser Scanning (TLS) surveys. A Leica HDS C-10 tripod mounted scanner can collect upwards of 50,000 points per second under ideal field conditions and has a field-of-view of 360 degrees horizontal and 270 degrees vertical. The Leica C-10 utilizes a single return pulsed based green laser (535 nm), which returns three-dimensional x, y, z and intensity (i) values for each laser pulse on the basis of the time of flight, angle of return, and albedo of the surface. The C-10 is a medium range laser scanner with a maximum range of 300 meters. Leica HDS planar reflective targets are used to create a series of reference points between multiple scan positions. The targets allow the data collected at multiple scan positions to become seamlessly integrated into one point cloud through the registration process.

The Root Mean Square Error (RMSE) and the Standard Deviational Error (σ) of the surveys were propagated throughout the scan series (Staley et al., 2011; Staley et al., *under review*). Our analysis of the DEM uncertainty provides a global error measurement based on local control points at the study site. The propagated error budgets for the x, y, and z values were calculated in order to assess the level of error associated with the scan data and to be able to

assign error at the individual pixel level. Pixel error is then used to give a ± value for the volumetric measurements. For the surveys collected at the study site the propagated RMSE = 8.3 mm and the σ error = 8.5 mm. Both error measures display sub centimeter error associated with the scan data. The σ error measures will be used at the pixel level in order to provide a conservative level of error assessment in the volumetric changes measurements.

Vegetation Filtering and DEM Generation

Geomorphic changes can only be accurately quantified between multiple scan series if the TLS data represent a bare earth model of the blowout surface. The computer software LAStools was used in this study to filter the excess vegetation allowing for the creation of bare earth models. LAStools was originally designed as a filtering program for airborne LiDAR; however, its ability to compress large amounts of data into usable .las files makes it ideal for handling the voluminous data recorded via TLS. Point cloud data are filtered through a series of coded command sequences that separate the ground and above ground data. A final step in the filtering process is to thin the data, while at the same time keeping the lowest points. This is done for two specific reasons: the first is to remove any artifacts of vegetation that would overestimate the bare earth surface and the second is to produce an initial point cloud with consistent point spacing to remove the potential for large spatial errors in the conversion of the points to a digital elevation model.

The filtered point cloud is then exported to ArcMap where it is converted into a raster grid. A 10 cm raster size was chosen in order to reduce the influence of residual artifacts in the data due to vegetation while still maintaining a high level of spatial resolution. Micro relief features such as grain avalanches, ripples and footprints are still visible, while stubble from the

remnants of individual grass stalks are removed. From here the DEM can then be transformed into various surface representations that aid in further study of the blowout geomorphology (e.g. slope mapping, curvature, hill shade etc.).

A total of five repeat geographic surveys were collected at the study site between May 2011 and May 2013. Two data sets exist displaying annual change (i.e. May 2011 – May 2012 and May 2012 – May 2013). The second year of the study multiple seasonal surveys were conducted including May 2012 – October 2012 (summer), October 2012 – November 2012 (fall), and November 2012 – May 2013 (winter). These annual and seasonal geo-datasets will be used to identify geomorphic changes occurring between subsequent scan surveys.

Global Geomorphic Analysis

The geomorphic evolution of the blowout is analyzed using the gross areal and volumetric changes taking place between successive pairs of scan surveys. In order to evaluate changes occurring in different parts of the blowout, a polygon is created that delineates the blowout rim, separating the erosional inner trough from the depositional outer lobe. The morphometry of the rim will be monitored in order to detect growth or reduction of the blowout feature through time. These rim and depositional lobe polygons are then used to quantify the areal and volumetric changes within each scan series.

Areal changes occurring within the polygons become the basis of monitoring the extent (m^2) of these features both spatially and temporally. Curvature and hill slope maps help identify the boundaries between the blowout and depositional lobes. Difference surfaces are generated from successive scan surveys in order to generate changes in elevation. These are then converted

to volumetric changes (m^3), based on the 10x10 cm pixel size, allowing for the sediment flux of the blowout and depositional lobe to be monitored.

Sub Landform Geomorphology

Geomorphic sub-landform zones are mapped in order to identify areas of the blowout surface that display homogeneity in terms of slope, directionality of slope, and field observations. Five commonly used descriptive zones in the blowout literature including the deflation basin, lateral slope, throat, transport ramp, and scarp will be used to classify the surface of the blowout. An area of reduced slope on the upper lateral wall was identified in both the field and the DEM and is classified as the shelf zone. The DEM will be used to generate a slope map that will be classified into ten Jenks Natural Break classes. Directionality of slope is also a factor when defining zones, for example, the transport ramp maintains a gradual slope extending parallel through the axis of the blowout while the lateral walls extend perpendicular away from the blowout axis. Finally field observations are used to calibrate the slope groupings and maintain a level of accuracy during classification.

The ranges of the slope used to classify the sub-landform geomorphic zones for each feature group include the throat 0-12.57°, the deflation basin 0-17.91°, the lateral slope 23.26-33.3°, the transport ramp, 6.92-23.25°, the shelf 12.58-23.25°, and the scarp zone >33.3° (Fig. 10). Some zone classes overlap in terms of slope, but the directionality of each zone also becomes a variable when deciding a classification. For example, the deflation basin and transport ramp have two different trending surfaces with the deflation basin slope creating a bowl while the transport ramp is a consistent gradating slope from the basin edge to the crest parallel through the axis of the blowout. Observations in the field and images taken by the scanner help

classification of these geomorphic zones. This is evident when identifying the scarp zones in which exposed roots and organic debris help to maintain a zone around the rim often exceeding the angle of repose for dry sand (i.e. >34°) and the transport ramp where ripples often extend the length of the feature.

These zones will be broken down further into areas of deposition and erosion in order to determine the dynamics of each zone as it pertains to dominant trends in sediment flux. The area of each zone is used to normalize the total amount of erosion and deposition in each geomorphic zone. This allows for the comparison of the zones in order to determine the individual rates of erosion and deposition. This will compliment the global volumetric changes by analyzing the spatial variability of volumetric changes occurring at the sub-landform scale providing insight into the geomorphic dynamics of each classified geomorphic zone.

Sediment Drift Analysis

The Sand Drift Potential model (Fryberger and Dean, 1979) was designed to analyze modal wind variation and potential sediment drift in desert dune environments based on regional wind data and remotely sensed imagery. This model will be here to analyze the level of localized topographic steering occurring in the blowout by comparing the results of potential sediment drift to the results from the repeat scan surveys. Wind records for the intervals between the scans were obtained from National Climatic Data Center for the Provincetown Municipal Airport weather station, located one kilometer southwest of the blowout. The original data has 36 directional classes that will be converted into 16 directional classes

The Sediment Drift Potential model (Fryberger and Dean, 1979) is based on several key assumptions including having a dry surface, free of vegetation, and having bed forms no larger

than mega ripples. Two modifications outlined by Pearce and Walker (2005) will be used to reduce magnitude bias in the Sediment Drift Potential model including using whole knots when defining the knot classes (e.g. 22-27.99 knots as opposed to 22-27 knots) and using the statistical mean of the winds in each wind class as opposed to the midpoint.

The Sediment Drift Potential model uses a modified version of Lettau and Lettau's (1975) sediment drift formula:

$$Q \propto V^2 (V - Vt) * t$$

Where Q represents the potential for annual sediment drift, V is the wind velocity (m/s) at a given height above the surface, Vt is the threshold wind velocity (m/s) with sand feed in, and t is the percentage of time the wind blew for each class. This is a weighted formula that takes magnitude and frequency into account when calculating drift potentials (DP). DP's are derived from this equation and are represented by Vector Units (VU) and the potential of sediment drift for 16 directions is used to qualitatively classify the study region as low (DP<200), moderate (DP= 200-399), or high-energy environments (DP≥400). From these VU's you can determine the resultant drift direction (RDD) or the general direction sediment is expected to drift and a resultant drift potential (RDP) which looks at the total magnitude based on the influence of multidirectional winds on sediment drift.

Before Q can be calculated the shear velocity must be determined from wind speeds recorded at 10 m above the surface. Fryberger and Dean (1979) used Belly's (1964) shear velocity for desert sand (30mm); however, this would not be analogous to the study site and must be modified according to on-site sediment characteristics. Bagnold's (1941) equation will first be used in order to determine the threshold shear velocity at the surface:

$$U * t = A \sqrt{\frac{\sigma - \rho}{\rho} g\, d}$$

Where $U * t$ is the threshold shear velocity, A is a coefficient that Bagnold (1941) approximated to be 0.1 for grain sizes >.25 mm, σ is the specific weight of quartz sand, ρ is the specific weight of air, g is the acceleration of gravity, and d is the diameter of the sand grains.

Bagnold's (1941) equation is then used in order to estimate the threshold velocity at a given height above the surface in order to maintain sediment transport. Zingg's (1954) estimation of the focus height and velocity will be used in this equation solving for Z' and U'.

$$U(10m) = C\ \log\frac{Z}{Z'} + U'$$

$$Z' = 10\ d\ (mm)$$

$$U' = 20\ d\ (mph)$$

Where $U(10m)$ is the threshold velocity at 10 meters above the surface (in this case ten meters is used because it is the standard height of the weather station's wind recordings). C is a coefficient theorized by Bagnold (1941) where *(2.3/K) U*t. K* represents Von Karman's constant (1934). Z is the height above the surface and Z' is the focus height estimated using Zingg's equation (1954) that represents the height at which mega ripples form across the surface accounting for surface roughness (Belly, 1964). U' is the velocity at the 'focus height' that is estimated using Zingg's equation (1954).

The Sediment Drift Potential model compared to observed sediment drift on-site provide a basis to determine the level of localized topographic controls on regional wind patterns. The

model results are compared to volumetric changes across half meter wide transects in the same 16 directions radiating away from the blowout centroid. The difference surface raster cells were sampled from the centroid and extending to the rim, giving total volumetric changes along these transects. The volumetric changes will be analyzed in patterns of deposition and erosion. The grand mean, a weighted circular statistic, is calculated in order to compare the directionality of actual sediment drift compared to the RDD determined using the Sediment Drift Potential model (Fryberger and Dean, 1979). Also the environmental energy classification gained from the DP values is compared to the activity across the surface during the study. These measurements provide a context by providing an understanding of the regional wind regime in relation to the geomorphic changes being observed on site.

In October 2012, a total of 12 sediment samples were collected in various locations across the active surface of blowout. The median grain size of .707 mm, which is classified as coarse sand, was used to determine the threshold velocity. The median value was chosen because the data were skewed due to sample #5, which was taken on the crest of a mega ripple (1.41 mm) and is unrepresentative of the larger sampled blowout surface. According to Bagnold's equation (1941) the threshold velocity at the surface is 26 cm/s. The shear velocity at 10 m above the surface, to maintain sediment transport, is 11.03 m/s. This was converted to 21.44 knots in order to be used in the Sediment Drift Potential model. This shear velocity was rounded up to the next wind class of 22-22.99 knots to be used as the minima competent wind class. All average wind speeds for the lower class (i.e. 17-21.99 knots) were below the threshold of 21.44, further providing justification to round up to the next higher class. The time period between May 2012 and October 2012 experienced only three observations slightly exceeding the threshold of 22 knots, and this data set was excluded in this analysis.

Results

Global Geomorphic Changes

Rim Morphometry

During the initial survey in May 2011, the study blowout consisted of a large horseshoe shaped trough blowout with an axis extending from the northwest to southeast. During this time a secondary feature, an incipient or embryo bowl blowout, had developed on the lee of the crest in the southern section of the rim. The baseline survey shows a clear ridge separating the blowout and its embryo dune (Fig. 3). A year later in May 2012 the ridge had eroded leading to an expansion of the blowout (Fig. 3). Over the course of a year, the total area of the blowout had increased by 563.27 m² or just under 28% of its original area (Fig. 3). The capture of the embryo directly led to 72% of the total areal increase of the blowout; and following this capture the ridge of the former embryo rapidly eroded leading to further expansion of the newly coalesced features. Between May 2012 to October 2012 the area of the blowout increased slightly by .37% (Fig. 3) over the summer months to 2521.08 m². During this time only small scale erosion took place in the scarp areas of the northwest and southeast sections of the rim, mainly the result of grain avalanching along scarped surfaces near the rim. One month after the October scan in November 2012 the blowout was resurveyed after the remnants of two major storms impacted the study site. The rim was constricted during this time period decreasing in size by .73% (Fig. 3) to 2502.6 m² as a ridge was deposited windward of the rim in the southeast section of the blowout. May 2013's survey once again showed expansion as the feature became more elongated up and down wind parallel to its axis during the winter months. The ridge that was deposited

following the storm events was removed leading to an increase in the blowout's total area by close to 5% to 2627.48 m^2 (Fig. 3).

Annual Elevation Change

During the first year of the study from May 2011 to May 2012 the surface of the blowout was dominated by erosion extending parallel through the axis (Fig. 4).There was a net erosion of 634.4 ± 20.5 m^3 (Fig. 4). The failure of the ridge that separated the study blowout and its embryo led to a large amount of sediment available for transport (Fig. 5). The capture led directly to major erosion around the rim and scarped areas of the former embryo bowl as high magnitude winds became funneled through this newly exposed area. This becomes evident in the DEM as ripples, indicating high wind speeds; extend just pass the deflation basin up through the newly captured embryo dune.

The second year of the study from May 2011 to May 2012 the majority of the surface experienced erosion with only localized areas of deposition (Fig.4). There was net erosion of 839.62 ± 22.26 m^3 (Fig.5) The total erosion is similar to the first annual survey, but overall the net erosion was higher due to the only localized low magnitude deposition. Localized areas of deposition were evident in the deflation basin and throat areas of the blowout (Fig 5). The deflation basin was actively eroded during the first survey but it appears to be stabilizing during the second year. Most of the erosion is centered through the primary axis in the southeast section of the blowout as the blowout is becoming modified following the capture of the embryo dune.

Vixen	Total Area m²	Areal Change m²	Expansion Rate
11-May	1948.59	N/A	N/A
12-May	2511.86	+563.26	28.91%
12-Oct	2521.08	+9.23	0.37%
12-Nov	2502.6	-18.48	-0.73%
13-May	2627.48	+124.88	4.99%

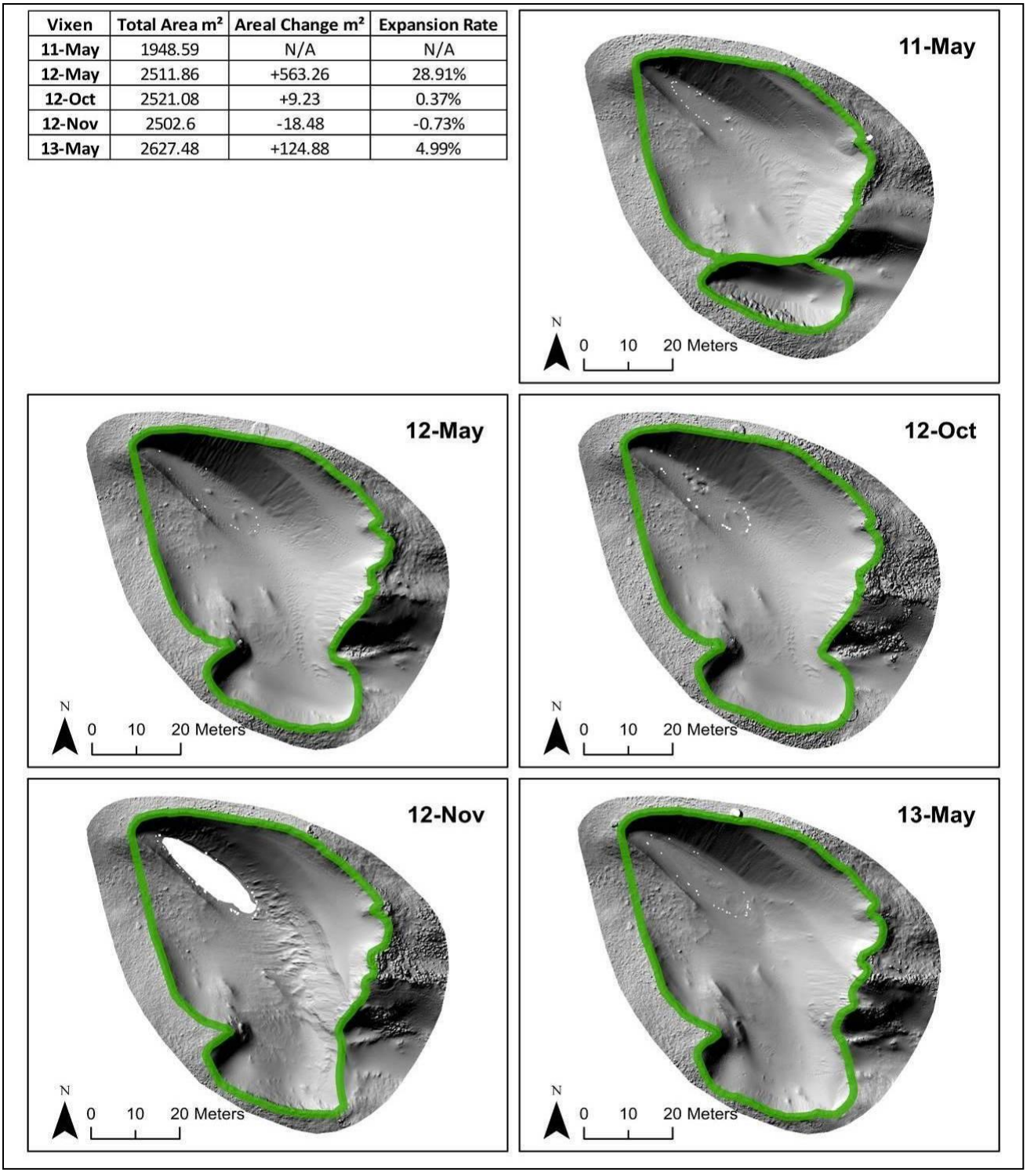

Figure 3: The area of the blowout is monitored through the changing rim polygons in terms of area, total expansion, and expansion of the blowout throughout the study. This expansion is displayed via the rim polygon maps.

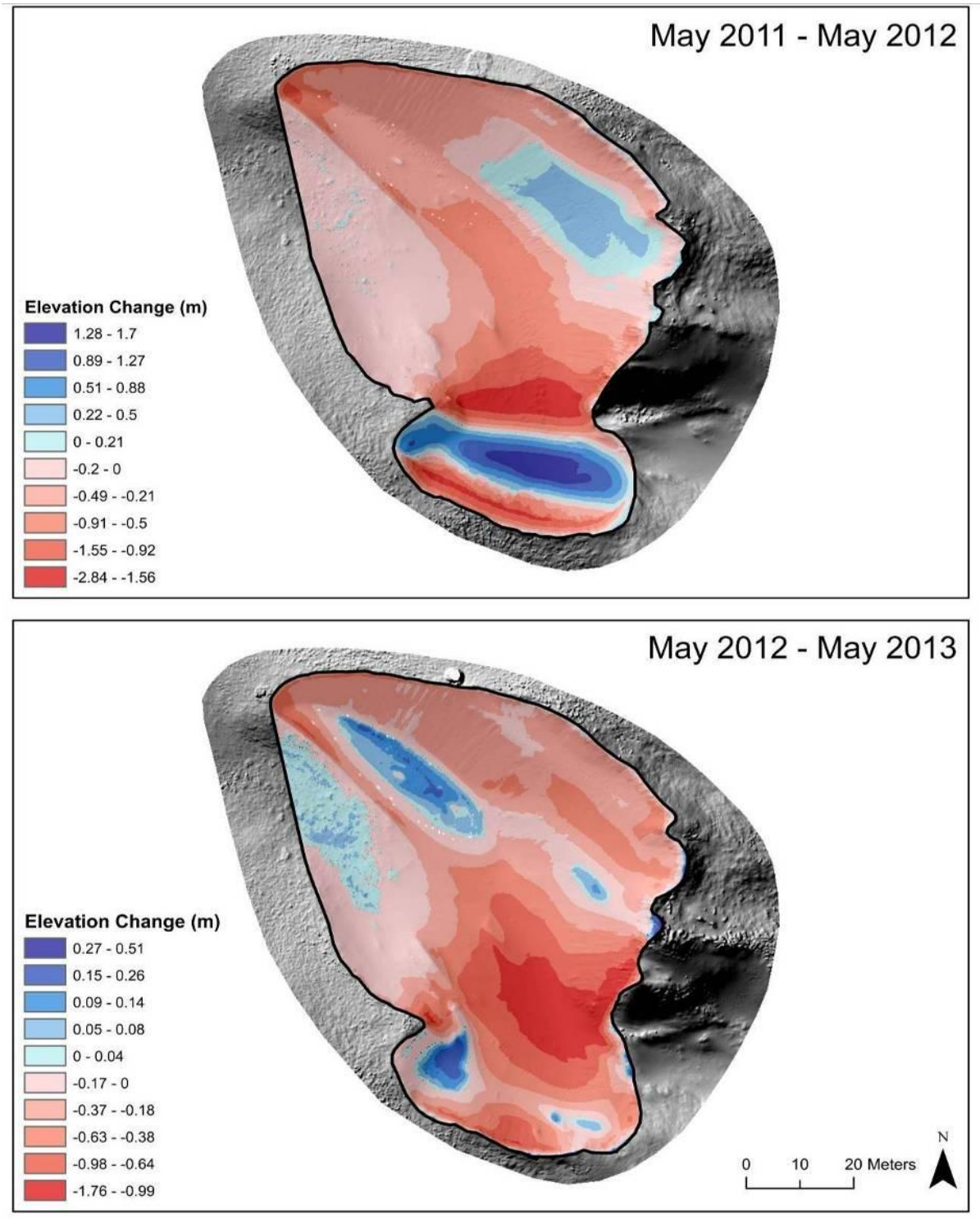

Figure 4: Difference rasters displaying the surface elevation changes between the annual scan surveys.

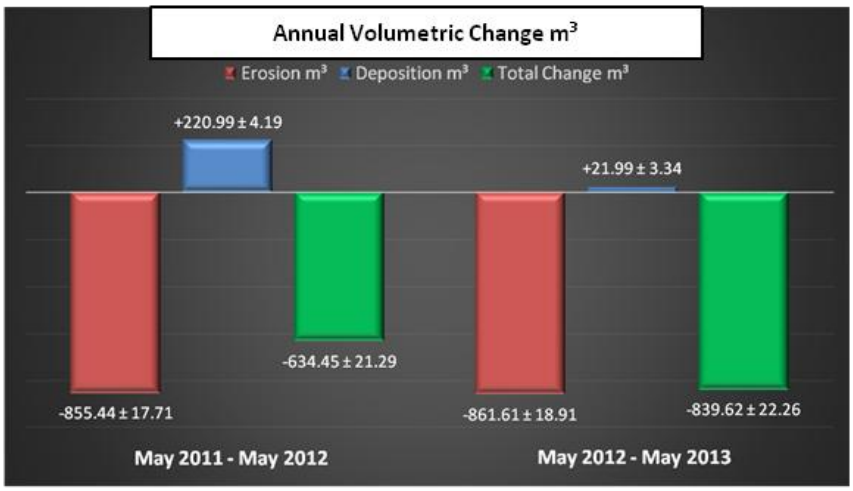

Figure 5: Total erosion, deposition, and net changes in m³ during the annual temporal scale.

Seasonal Elevation Change

Following the May 2012 topographic survey the study site was resurveyed in October 2012 and would be representative of a summer seasonal temporal scale. There was a net deposition of 29.2 ± 20.5 m³ (Fig. 6) during this time period as low magnitude non-axis parallel winds over the summer led to a period of relative inactivity. Only small volumetric changes were recorded. The majority of the surface was dominated by small amounts of deposition with a few small areas of erosion associated with avalanching in the scarp areas near the rim of the blowout (Fig. 6). The error for this survey becomes more pronounced given the majority of deposition is <2 cm per pixel. The standard deviational error assigned to each pixel was close to 8 mm and led to more uncertainty in the volumetric measurements during this time period.

One month following the October survey the blowout was resurveyed in November 2012 and would be representative of a fall seasonal temporal scale. Two known storm events impacted the study site during this time and substantial changes were recorded with a net erosion of 166.1

± 19.4 m^3 (Fig. 6). A large amount of sediment was scoured out through the transport ramp up the axis of the blowout as well as large amounts of sediment deposited on the upper slopes of the western lateral wall (Fig. 6). The deposited material was still saturated from intensive rainfall and was temporarily stabilized at a slope exceeding the angle of repose of dry sand. Extensive avalanching was seen following the survey as the surface began to increase in aridity due to increased solar radiation. The high water table inundated the deflation basin causing this area to flood and leading to data voids in the DEM (Fig. 6) making the full volumetric changes associated with the storms unknown.

The study blowout was resurveyed in May 2013 and this time period will be used to determine changes associated with a winter seasonal temporal scale. Major erosion occurred across the majority of the active surface of the blowout leading to a net erosion of 736.5 ± 20.5 m^3 (Fig. 6). The most prominent erosion surfaces occurred through the main axis of the blowout and the lateral slope. Small areas of deposition occurred around the deflation basin and a remnant deflation basin in the capture embryo bowl (Fig. 6). The data void in the previous scan doesn't allow for the elevation change to be recorded in the deflation basin.

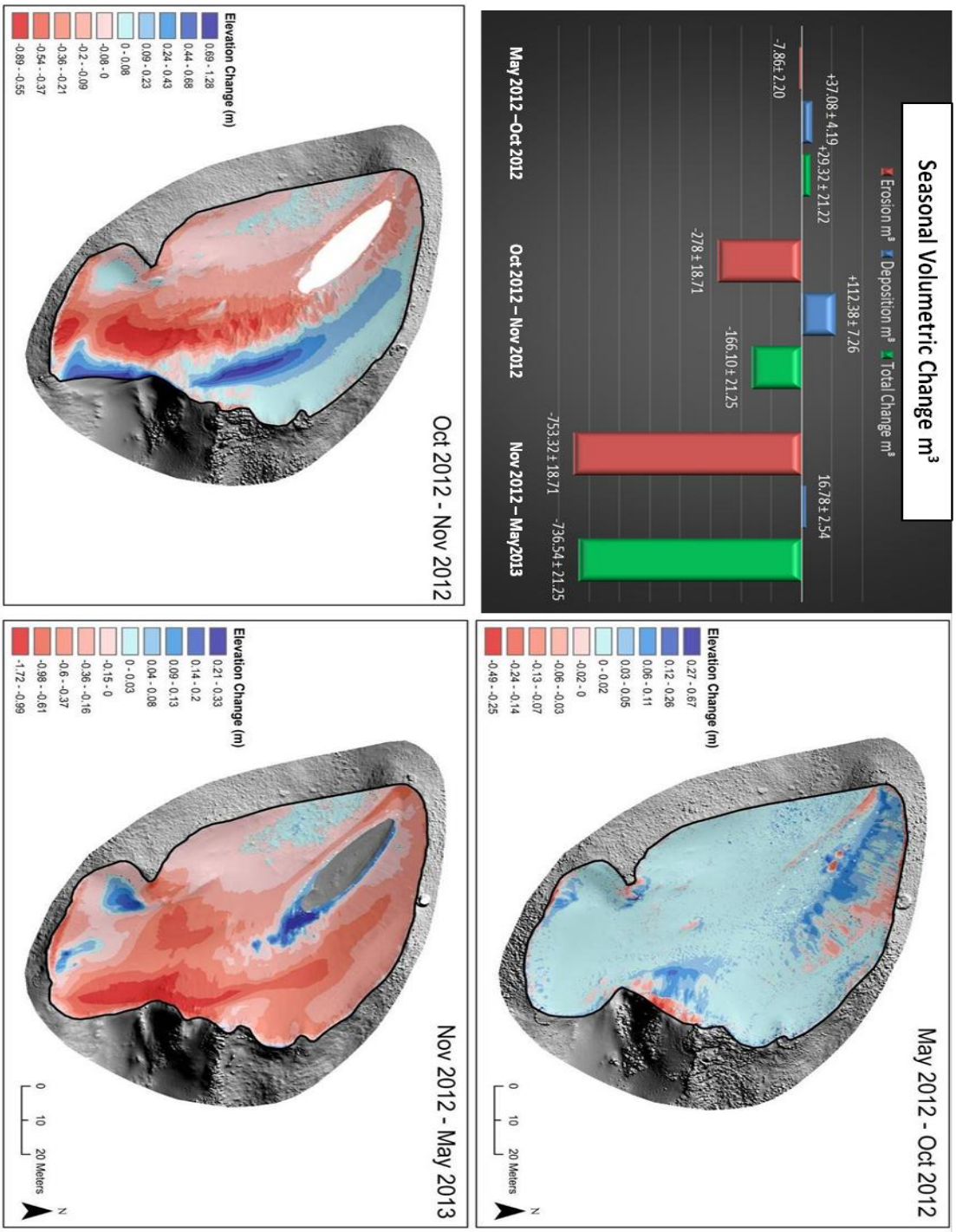

Figure 6: Volumetric changes occuring at the study site and difference rasters displaying the surface elevation changes.

Annual Depositional Lobe Elevation Change

Two primary depositional lobes were identified both in the field and in the DEMs, but the areal extent of these features appeared to change little. Areal changes over time will not be analyzed due to this uncertainty and the largest extent of the known depositional lobes will be used to determine the amount of deposition at the site during all time series. During the first year from May 2011 to May 2012 there was both noticeable deposition and erosion occurring on the lee of the rim in the southeastern section of the blowout (Fig. 7). There was 178.5 ± 13.5 m^3 of deposition but a net change of 88.64 ± 24.83 m^3 of erosion (Fig. 8). As ripples extend through the captured embryo dune, it appears to be steered towards the west and could be the cause of intensive erosional streamers occurring during this time period. The full extent of the depositional lobe was not captured in the May 2011 scan, allowing for only partial changes to be monitored during the first year.

The second annual survey shows deposition across the majority of the lobe surface (Fig. 6). Areas of erosion occur in the same pattern as the first year but are of lower magnitude. There was a total of 615.88 ± 22.26 m^3 of deposition (Fig. 8). High magnitude deposition was focused around the southeast extent of the depositional lobe (Fig. 7). As airflow was modified by the expansion of the rim, deposition became intensified in the lee of the former embryo dune. This suggests airflow is becoming funneled through this area and remaining attached causing continuous erosion. This was qualitatively observed during the first annual survey by the formation of ripples extending through this relict feature. Funneling of airflow may lead to the continued expansion of the depositional lobe in the south and southeast section and our annual observations support this.

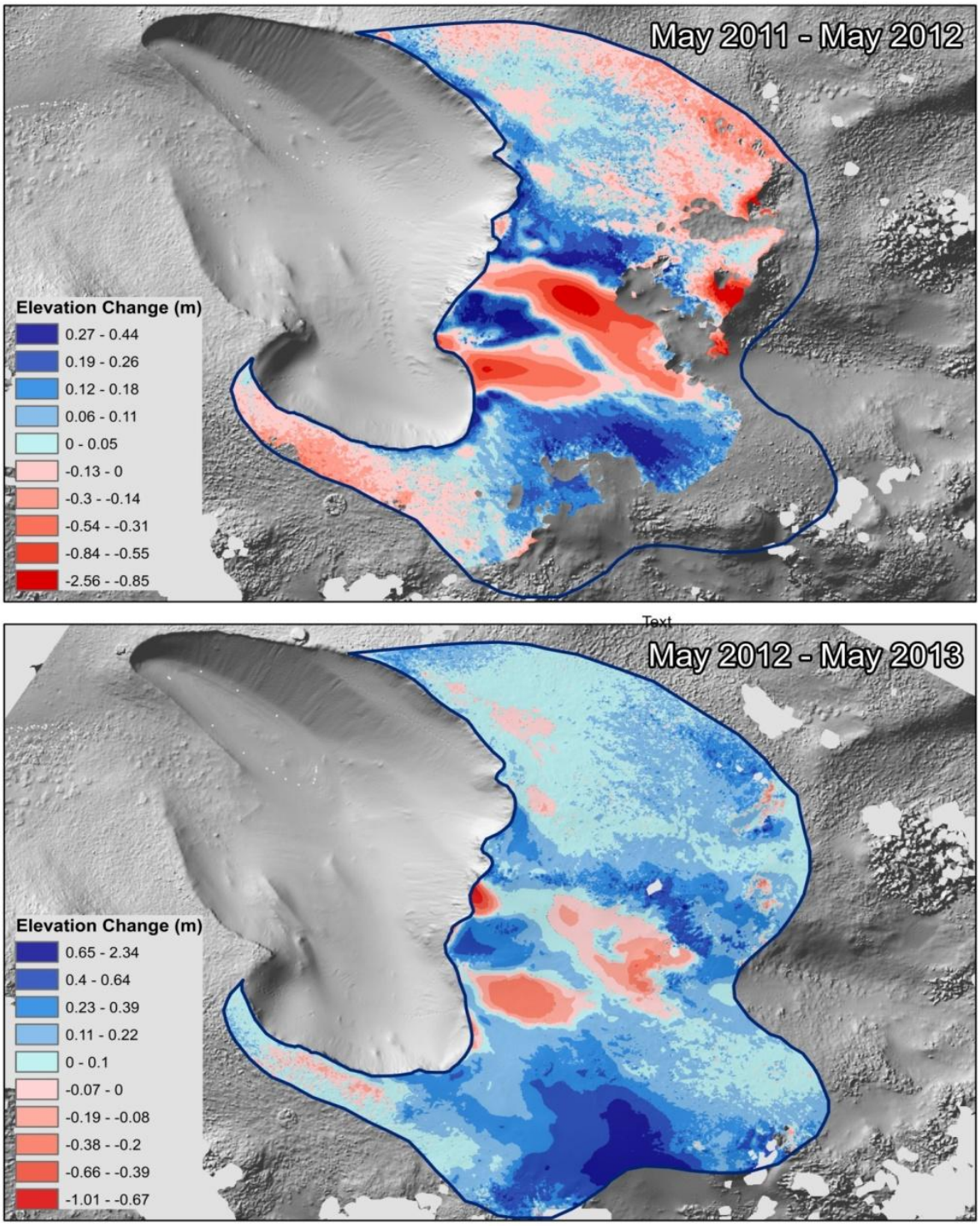

Figure 7: Annual elevation changes on the depositional lobe.

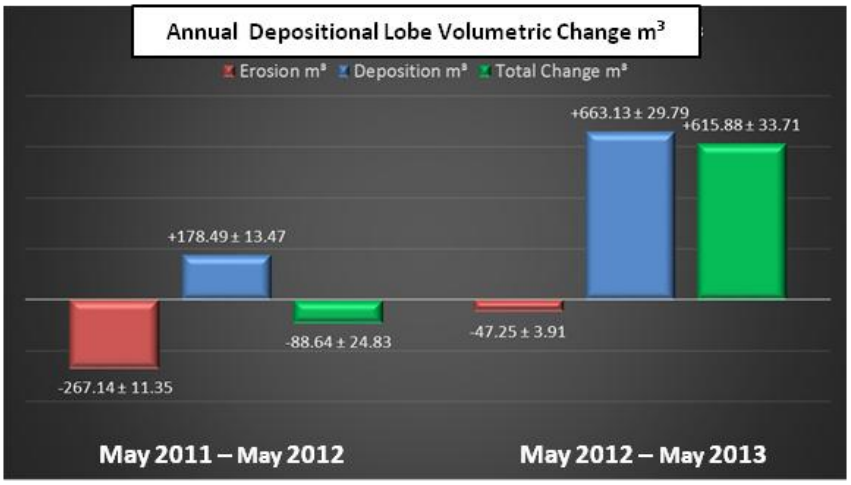

Figure 8: Annual volumetric changes on the depositional lobe.

Seasonal Depositional Lobe Elevation Change

Over the summer months (i.e. May 2012 – October 2012) there was deposition recorded across the majority of the depositional lobe surface (Fig. 9). Only small areas of erosion were observed on the lee of the rim as well as some minor areas of erosion downwind. There was a net of 333.88 ± 28.64 m³ of deposition during this time period. Areas of dense vegetation were excluded by removing data that was two standard deviations away from the mean distribution. This removed values that were located in the 'faceted' areas of the DEM. These facets represent areas of dense vegetation that inhibited the collection of true ground points through TLS. On the fringes of the densely vegetated areas there are higher levels of deposition; however, it is unknown the level of deposition occurring in the densely vegetated areas.

The fall seasonal survey, conducted in November 2012, recorded erosion across the majority of the depositional lobe surface (Fig. 9). Erosional values overestimated the loss in elevation because the loss of the transition from a densely vegetated surface to a sparsely vegetated surface. Erosional values exceeding two standard deviations away from the mean were

excluded to remove values that represented this loss in vegetation. There was intensive deposition on the lee of the crest in the southeast section of the blowout rim. This corresponds to the rim morphometry during this time period. The area of the blowout was restricted due to a ridge of sediment being deposited in this area and the deposition continues directly downwind on the depositional lobe. There was 117.41 ± 10.80 m^3 of deposition but a net of 161.06 ± 23.69 m^3 of overall erosion (Fig. 9). Two major storms impacted the study site in this time period leading to widespread erosion across the depositional lobe. Deposition was restricted downwind of the rim parallel to the intense scouring of material occurring within the blowout.

During the winter months (i.e. November 2012 – May 2013), the depositional lobe experienced intensive deposition and erosion (Fig. 9). There was a net of 144.86 ± 32.03 m^3 of deposition during this time period. Erosion is once again observed in the lee of the crest in the southeast section of the blowout. This section of the rim is topographically low in comparison to the surrounding rim crests. Airflow likely remains attached and steered through this area becoming compressed as it passes through the rim.

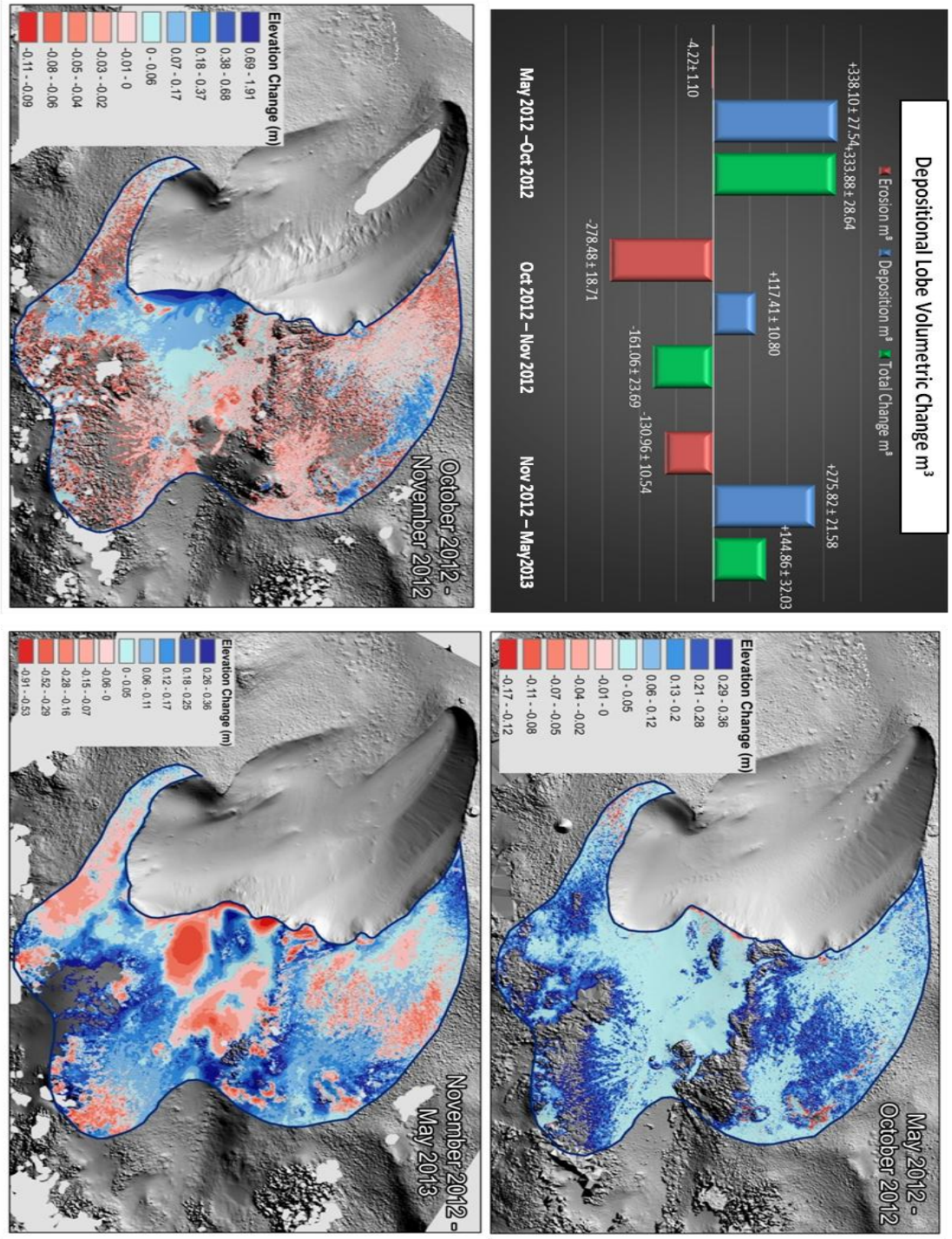

Figure 9: Seasonal Volumetric changes on the depositional lobe and elevation change maps.

Sub Landform Geomorphology

Annual Volumetric Changes

The first year of the study May 2011 to May 2012 experienced net erosion in all of the geomorphic zones. The transport ramp had the most volumetrically active surface with a net erosion of 358.08 m^3 (Table 1). This zone extended through the axis to the rim of the former embryo leading to large amount of erosion following the embryo dune capture. The lateral slope (135.56 m^3), scarp zone (75.44 m^3), deflation basin (47.54 m^3), and throat (17.7 m^3) all were actively eroding during the first year of the study. The shelf zone had equal levels of deposition and erosion during this time period displaying a net change of only 0.3 m^3 of erosion (Table 1). When comparing the volumetric changes in these zones per unit area, the transport ramp has the highest volumetric change per unit area (Table 1). While contributing less total volumetric change then the transport ramp and lateral slope, the scarp (-.41) and deflation basin (-0.36) have the next highest levels of erosion per unit area (Table 1).

May 2011 - May 2012	Area m^2	Erosion m^3	Deposition m^3	Net Change m^3	Change Per Unit Area
Lateral Slope	670.0	-135.7 ± 4.0	38.1 ± 1.7	-97.5 ± 5.7	-0.15
Scarp	183.3	-75.5 ± 1.5	0.1 ± 0.0	-75.4 ± 1.6	-0.41
Deflation Basin	131.1	-47.5 ± 1.1	0.0 ± 0.0	-47.5 ± 1.1	-0.36
Shelf	49.1	-7.6 ± 0.2	7.4 ± 0.2	-0.3 ± 0.4	-0.01
Transport Ramp	687.9	-359.1 ± 5.8	0.2 ± 0.1	-358.9 ± 5.8	-0.52
Throat	225.9	-17.7 ± 1.9	0.1 ± 0.1	-17.7 ± 1.9	-0.08

Table 1: Sub-landform dynamics during the first annual survey.

The second annual survey shows the expansion of all geomorphic zones except for the throat zone (Table 2.). The transport ramp and lateral slope have the highest total volumetric changes with 428.4 m^3 and 245.6 m^3 of erosion respectively. Per Unit area the transport ramp (-0.50) and the scarp (-0.44) displayed the highest level of change based on the areal extent of these features. The results in comparison to the first annual survey provide similar results except for the deflation basin and the shelf zones (Tables 1 and 2). The deflation basin appeared to become stabilized in the DEMs and the sub-landform analysis supports this. The first year of the survey the deflation basin had a net of 47.5 m^3 of erosion compared to the second year with only 5.7 m^3 of erosion. The shelf zone was largely balanced in the first year while the second year it shifted to a completely erosional feature (Tables 1 and 2).

May 2012 - May 2013	Area m^2	Erosion m^3	Deposition m^3	Net Change m^3	Change Per Unit Area
Lateral Slope	870.6	-245.6 ± 7.0	1.8 ± 0.4	-243.8 ± 7.4	-0.28
Scarp	242.1	-106.4 ± 2.0	1.0 ± 0.1	-105.3 ± 2.1	-0.44
Deflation Basin	225.5	-7.6 ± 0.6	13.3 ± 1.3	5.7 ± 1.9	0.03
Shelf	109.9	-31.5 ± 0.9	0.0 ± 0.0	-31.5 ± 0.9	-0.29
Transport Ramp	848.3	-428.4 ± 6.9	1.1 ± 0.3	-427.3 ± 7.2	-0.50
Throat	216.1	-9.8 ± 0.8	2.9 ± 1.0	-6.9 ± 1.8	-0.03

Table 2: Sub-landform dynamics during the second annual survey.

Seasonal Volumetric Changes

From May 2012 to October 2012 there was an overall trend of net deposition in all zones. The lateral slope and transport ramp had 12.9 m^3 and 9.9 m^3 of deposition respectively. These two zones accounted for the majority of deposition within the blowout totaling 72% of the net deposition (Table 3). Per unit area all zones had low levels of change (i.e. <0.02).The scarp and lateral slope recorded the highest amounts of erosion during this time period (Table 3). This was evident in the October DEM which showed grain avalanching originating in the scarp areas and the steep lateral wall.

May 2012 - October 2012	Area m^2	Erosion m^3	Deposition m^3	Net Change m^3	Change Per Unit Area
Lateral Slope	860.6	-1.8 ± 1.0	14.7 ± 6.3	12.9 ± 7.3	0.02
Scarp	238.3	-5.1 ± 0.8	5.4 ± 1.2	0.2 ± 2.0	0.00
Deflation Basin	224.7	-0.4 ± 0.1	4.5 ± 1.8	4.1 ± 1.9	0.02
Shelf	109.9	0.0 ± 0.0	1.3 ± 0.9	1.3 ± 0.9	0.01
Transport Ramp	843.8	-0.1 ± 0.2	10.1 ± 7.0	9.9 ± 7.2	0.01
Throat	216.1	0.0 ± 0.0	3.1 ± 1.8	3.0 ± 1.8	0.01

Table 3: Sub-landform dynamics during the summer season

The fall seasonal survey, November 2012, produced an overall trend of erosion in all zones except the shelf zone. The transport ramp recorded the highest amount of volumetric change with a net erosion of 163.59 m^3 followed by the scarp zone with erosion of 10.16 m^3 (Table 4). The lateral slope also had a large amount of erosion; however, this was counteracted

by the large amount of deposition occurring on the upper slopes. At this time period a linear ridge of sediment was deposited on the upper lateral slope leading to net deposition of 27.97 m^3 (Table 4). The transport ramp displays the highest level of erosion per unit area (-0.19) followed by the deflation basin (-0.06) and the scarp zone (-0.04). This provides an understanding of the response of geomorphic zones to major events and it appears to be a very dynamic surface with major erosion and deposition occurring in the more active zones (i.e. transport ramp, lateral slope, and scarp).

October 2012 - November 2012	Area m^2	Erosion m^3	Deposition m^3	Net Change m^3	Change Per Unit Area
Lateral Slope	900.9	-50.9 ± 3.5	78.9 ± 4.1	28.0 ± 7.6	0.03
Scarp	234.5	-15.4 ± 1.1	5.2 ± 0.8	-10.2 ± 2.0	-0.04
Deflation Basin	89.5	-6.0 ± 0.6	0.8 ± 0.2	-5.2 ± 0.8	-0.06
Shelf	110.3	-0.2 ± 0.1	4.6 ± 0.8	4.4 ± 0.9	0.04
Transport Ramp	843.3	-200.4 ± 6.3	36.8 ± 0.8	-163.6 ± 7.2	-0.19
Throat	227.4	-4.8 ± 1.3	0.6 ± 0.6	-4.3 ± 1.9	-0.02

Table 4: Sub-landform dynamics during the fall season.

Between November 2012 and May 2013 there was net erosion in all geomorphic zones. The lateral slope had the most erosion with 335.13 m^3 followed by the transport ramp with a net of 237.09 m^3 of erosion (Table 5). The scarp zone had the highest level of erosion per unit area (-0.39), while shelf (-0.38), transport ramp (-0.36) and lateral slope (-0.35) all had relatively high rates of erosion (Table 5). The deflation basin had a less active surface due to the large data void

from the November survey. The throat is the most inactive surface with small volumetric changes (-2.5 m^3) occurring in this zone (Table 5). The deflation basin also had the highest rate of deposition in large part due to the remnant deflation basin in the former embryo, which is included in the volume measurements. Erosion dominated the surface and deposition was relatively minimal during the winter season. The winter seasonal changes are more analogous to the annual changes taking place within the geomorphic zones.

November 2012 - May 2013	Area m^2	Erosion m^3	Deposition m^3	Net Change m^3	Change Per Unit Area
Lateral Slope	911.7	-316.6 ± 7.5	1.5 ± 0.2	-315.1 ± 7.7	-0.35
Scarp	253.1	-99.6 ± 2.0	1.1 ± 0.1	-98.5 ± 2.1	-0.39
Deflation Basin	225.9	-16.5 ± 1.0	10.5 ± 0.9	-5.9 ± 1.9	-0.03
Shelf	110.5	-42.1 ± 0.9	0.0 ± 0.0	-42.1 ± 0.9	-0.38
Transport Ramp	768.0	-275.7 ± 6.1	2.6 ± 0.5	-273.1 ± 6.5	-0.36
Throat	243.4	-3.7 ± 1.2	1.1 ± 0.9	-2.5 ± 2.1	-0.01

Table 5: Sub-Landform dynamics during the winter season

Sediment Drift Analysis

Annual Sediment Drift

During the first year, the average regional wind direction was out of the southwest where high frequency lower magnitude winds predominate (Fig. 10). There were some major events (i.e. >11.03 m/s) detected from the southwest, west northwest, and northeast (Fig. 10). The Sediment Drift Potential model shows a bi-modal wind regime with a net DP of 0.52 and a RDP

of 0.19, which would classify this time period as low energy with competent winds occurring only 2% of the time (Fig. 11). The RDD is 99° given the influence of the events capable of transporting sediment (Fig. 11). The deposition during this time period was dominated in the South Southeast section of the blowout with a grand mean of 152°, which was shifted 52° from the predicted RDD. There was a net of 13.11 m^3 of deposition (Fig. 12). The erosion was dominated along the central axis of the blowout running northwest to southeast with a grand mean of 142°, which was shifted 43° from the predicted RDD (Fig. 13). There was a total of -84.37 m^3 of erosion (Fig. 13) displaying a highly active surface over the course of the annual temporal scale.

The average wind direction during the second year of the study was from the Southwest (Fig. 10). High magnitude events are visible from the northwest and northeast (Fig. 10) The Sediment Drift Potential model shows a bi-modal wind regime and there is a net DP of 1.88 and a RDP of 0.69 (Fig.11). During this annual period, the study site would be classified as low energy with competent winds occurring only 3% of the time. The RDD is 199° and predicts sediment to drift in a south southwest direction (Fig. 12). Deposition recorded during this time period was oriented towards the northwest with a grand mean of 332° (Fig. 10). A total of 0.91 m^3 of net deposition was recorded (Fig. 12). Erosion was again oriented towards the southeast and the grand mean is the same as the first year at 142° (Fig. 13). The overall volumetric erosion during the second annual survey was 82.04 m^3 (Fig. 13). The directionality of erosion remains the same between both annual time periods and the volumetric erosion varied only slightly.

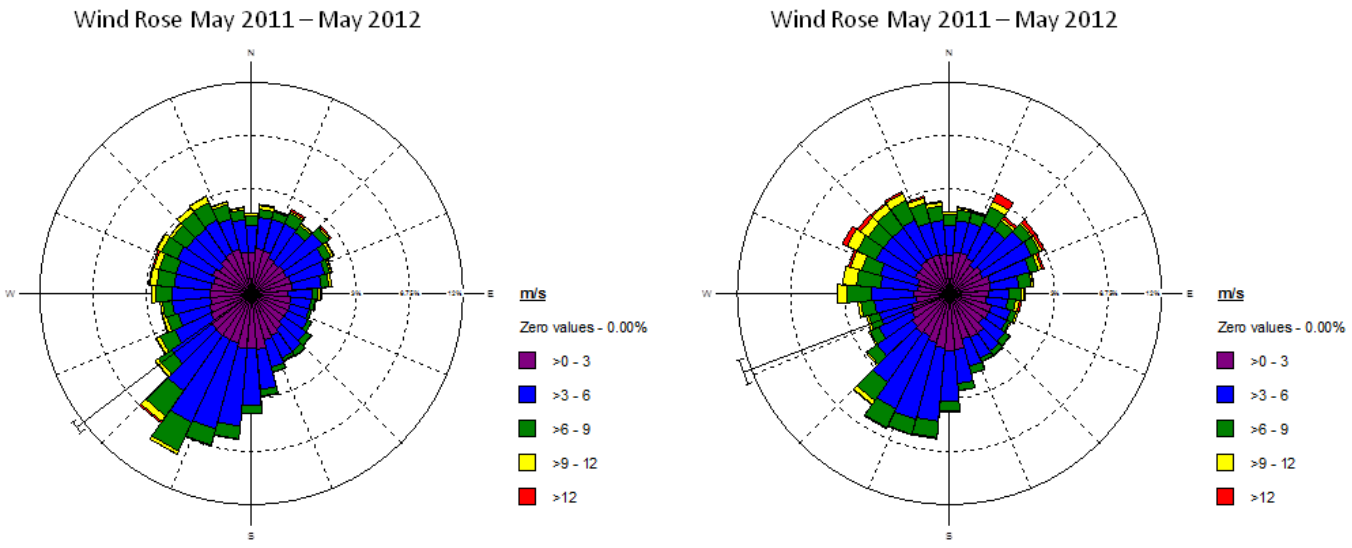

Figure 10: Wind roses that show regional wind patterns during the first and second year of the study.

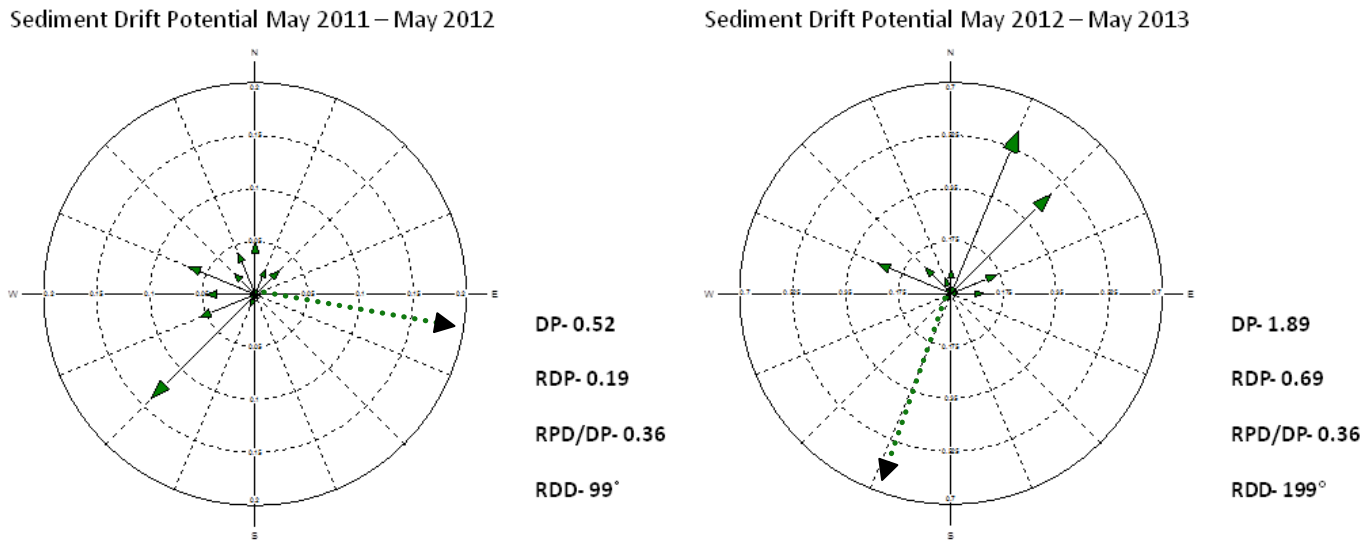

Figure 11: Sediment Drift Potential models showing (DP) and Resultant drift potential (RDP). The RDP/DP determines the modal variability in the wind regime. And the resultant drift direction (RDD) is the directionality of the expected drift of sediment being influenced by all competent winds.

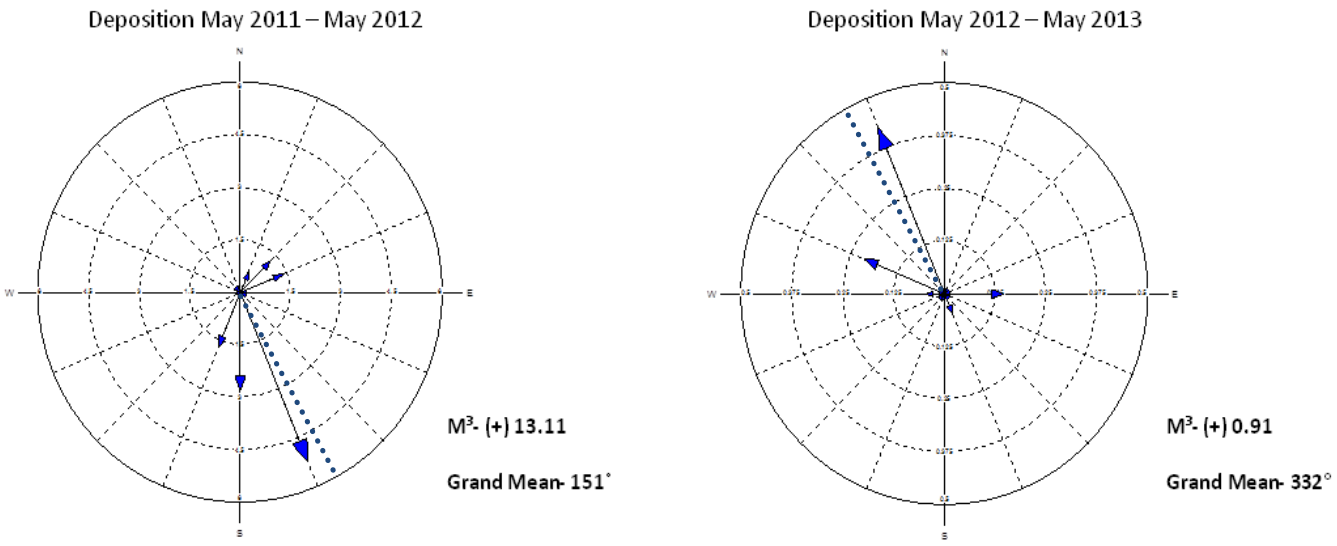

Figure 12: Direction and magnitude of deposition radiating away from the centroid in ½ meter wide transects during the two annual surveys.

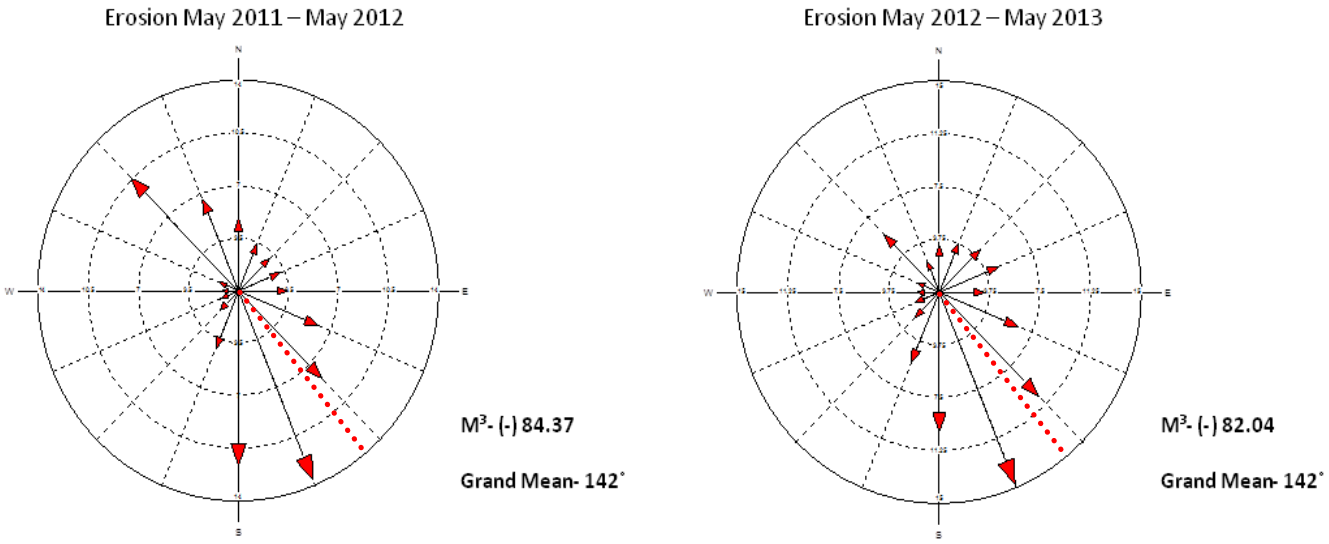

Figure 13: Direction and magnitude of erosion radiating away from the centroid in ½ meter wide transects during the two annual surveys.

Seasonal Sediment Drift

Average winds approached from the northwest during the period of October 2012 and November 2012. However, two large storm events occurred with high magnitude winds coming from the north and northeast (Fig. 14). The Sediment Drift Potential model shows a bi modal wind regime with a net DP of 5.28 and RDP of 2.95, which classifies this time period as a low energy environment with competent winds occurring 7% of time (Fig. 14). The RDD for this time period was 117° predicting sediment drift to the southwest (Fig. 15). Deposition displayed a primarily west orientation with a grand mean of 79°, which shifted -149° off of the predicted RDD (Fig. 16). There was a net of 7.07 m^3 of deposition (Fig. 16) during this one month period across the 16 transects. Erosion dominated in the south southeast of the blowout, running through the primary axis of the blowout. The directionality of erosion had a grand mean of 139° (Fig. 17), which shifted from the predicted directionality of sediment drift by -89°. There was a total of -31.07 m^3 net erosion (Fig. 17) exhibiting intensive sediment drift during the event temporal scale.

Between November 2012 and May 2012, the average wind direction was from the west northwest with major wind events coming from the northwest and northeast (Fig. 14). There is a bi-modal wind regime with a net DP of 2.78 and RDP of 2.95 indicating a low energy environment with competent winds occurring 5% of the time (Fig. 15). The predicted sediment drift is slightly off south with a RDD of 191° (Fig. 15). Deposition occurred mainly oriented in a north direction with the grand mean of 10°, which shifted from the predicted drift direction by 179° (Fig. 16). There were only low levels of deposition with a total of 1.58 m^3 net deposition (Fig. 16) during this time period. The erosion was once again oriented towards the southwest with a grand mean of 127°, which shifted 64° off of the predicted directionality of sediment drift

(fig. 17). There was a total of -61.39 m³ of net erosion where large volumetric changes occurred during the winter seasonal temporal scale (fig. 17).

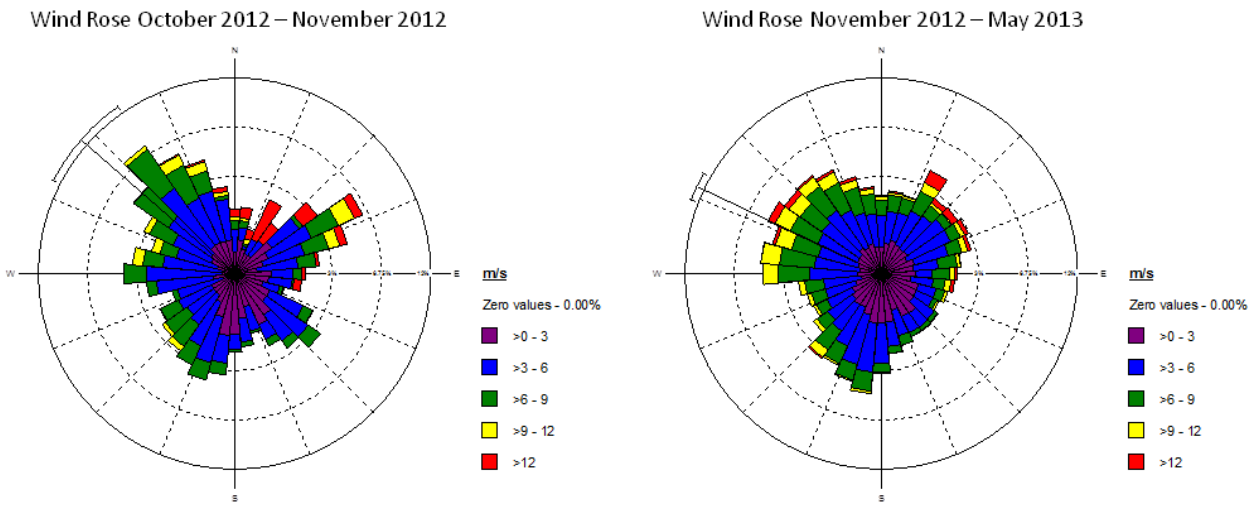

Figure 14: Wind roses that show the regional wind patterns during the fall and winter seasons.

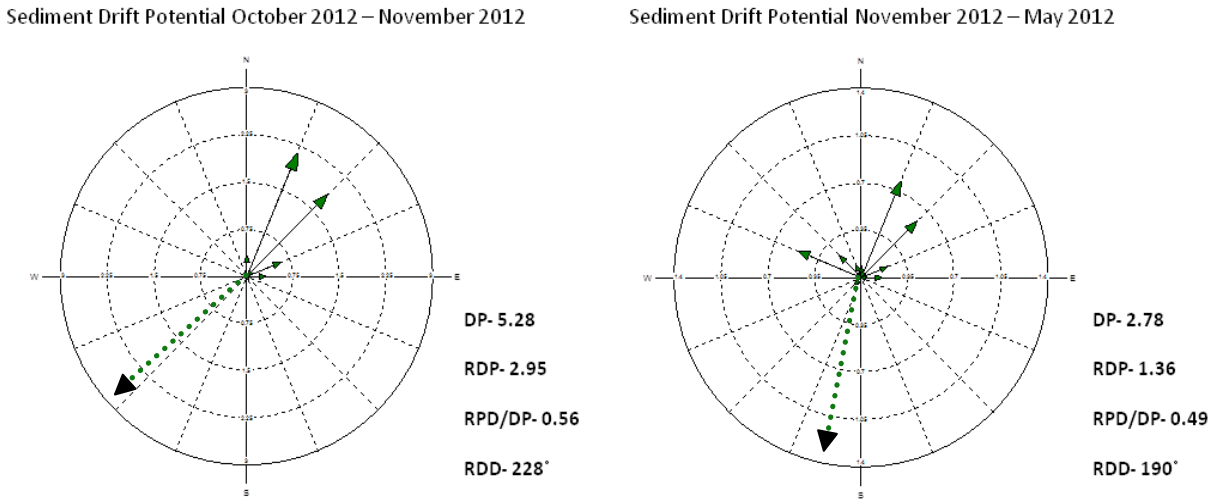

Figure 15: Sediment Drift Potential models showing (DP) and Resultant drift potential (RDP). The RDP/DP determines the modal variability in the wind regime. And the resultant drift direction (RDD) is the directionality of the expected drift of sediment being influenced by all competent winds.

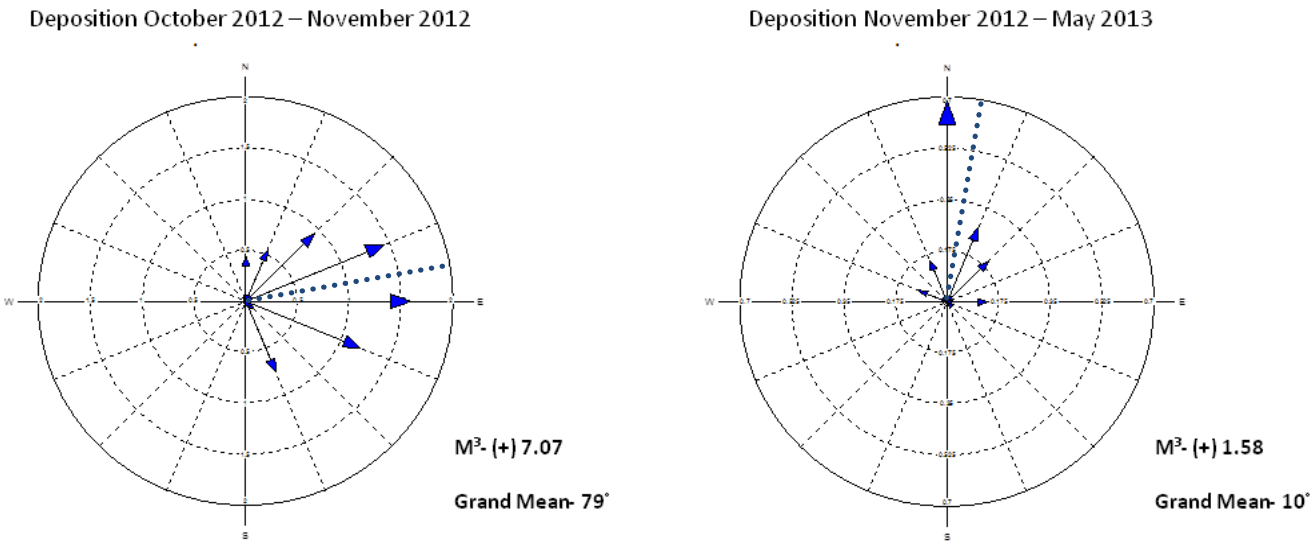

Figure 16: Direction and magnitude of deposition radiating away from the centroid in ½ meter transects during the two seasonal surveys.

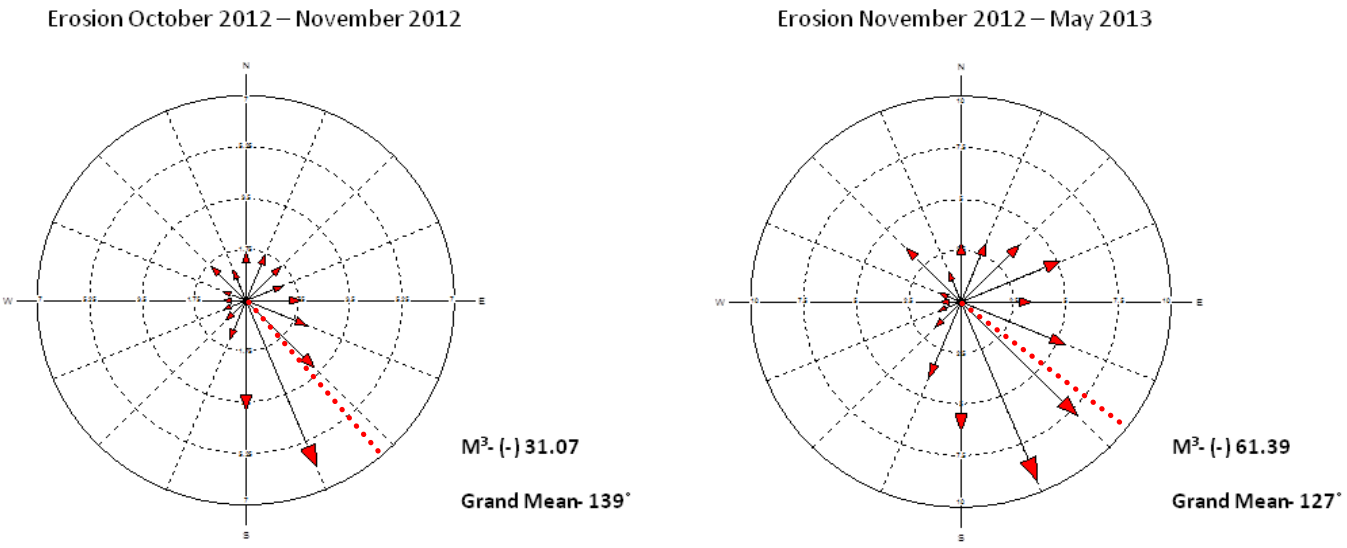

Figure 17: Direction and magnitude of erosion radiating away from the centroid in ½ meter wide transects during the two seasonal surveys.

Discussion

Global Geomorphic Changes

During the first year of the study the embryonic dune capture was the most significant expansion of the total area of the blowout. This mass expansion increased the total area by over a quarter of its previous size during a one year period. Incipient or embryo dunes have been identified in previous studies, but they have not been adequately studied in terms of their geomorphic significance. Jungerius and Van der meulen (1989) observed incipient blowouts only a few meters wide that developed on elevated ridges, however, their long term aerial photography analysis of the expansion of blowouts had a spatial resolution of 5 meters and could not monitor the small scale features through time. Advances in TLS allows for high resolution DEM's to be created in order to monitor changes of small scale features such as incipient blowout dunes, which portrays an important phase in the evolution of these features. While the capture at study blowout is only one example of embryonic dune capture, these features appear to be ubiquitous at Provincelands Dunes and need to be studied further in order to determine a different evolutionary understanding of the expansion of blowout dunes. They potentially provide a previously neglected form of blowout evolution by mass expansion attributed to rim failure and subsequent capture of embryo dunes by their host blowout.

The second year of the study experienced smaller changes compared to the previous year. During this time period blowout became more elongated up and downwind of the axis. Over the summer months, the rim expanded slightly as the scarp zones eroded via grain avalanching. Restriction of the rim was monitored during the fall season, due to extensive deposition of material creating a temporary rim in the southeast section of the blowout. This newly formed

ridge was subsequently removed during the winter months. The highest rate of rim expansion during the second year of the study was recorded following the winter and is likely more representative of changes occurring annually as the blowout rim eroded linearly along its longitudinal axis.

Large-scale annual volumetric changes were recorded at the blowout as both time periods experienced >800 m^3 of erosion. The study blowout is a large trough, but it maintains a high level of activity. The dynamic nature of the blowout suggests that it is not close to a critical threshold in terms of development. While it has been theorized that blowouts experience a cyclical cycle of initiation and stabilization (Gares and Nordstrom, 1995), the blowout appears to more resemble continental dunes where sediment supply is generated internally in a closed system (Hugenholtz and Wolfe, 2006). The first year saw a major geomorphic event in the capture of the embryo dune which introduced large amounts of erosion and deposition in the area of the relict feature. This capture appears to have increased sediment available for transport in the second year of the study. The net erosion was increased during the second year and was a result of intensified erosion in the southeast section of the blowout.

During the summer months, only small amounts of deposition was recorded across the surface with only small areas of erosion via avalanching near the rim. This suggests that low magnitude non-axis normal winds have little geomorphic implications for the evolution of the blowout. Volumetric changes following the winter months account for the majority of the annual volumetric changes at the study site. Winds during this time period are of higher magnitude and generally correspond more to the axis of the blowout. Hugenholtz and Wolfe (2006) found that seasonal climatic factors such as solar aspect have impact on the geomorphic evolution of

blowouts; however, the blowout's evolution appears to be driven by periods of high magnitude axis normal winds caused by increased storminess during the winter months.

The volumetric changes occurring in the fall months were recorded following the remnants of Hurricane Sandy and Nor'easter impacting the study site. Deposition occurred in a linear pattern on the upper lateral slopes of the blowout. This deposited material was likely generated internally due to scouring of the transport ramp. High magnitude winds which ranged from 350-100° were funneled into the blowout normal to its axis. This could have caused a jet flow with corkscrew vortices described by Hesp and Hyde's (1996) model leading to deposition on the upper slopes of the lateral wall. Field observations of intense scouring (Fig. 18) differed greatly from general field observations of axis parallel ripples that are expected during more laminar airflow. The ripples observed at this time period developed perpendicular to the axis and were found in the areas that displayed intense scouring. The region surrounding the blowout were largely stabilized and unlikely to have been able to generate enough sediment to have contributed the 112.38 ± 7.3 m^3 of deposition during this one month time period. This suggests that the deposition was generated internally through erosion of the transport ramp, which was then deposited on the upper lateral slopes.

Figure 18: A picture of the study blowout following two major storm events. Intense scouring extended through the axis of the blowout. Notice ripples extending perpendicular from the axis.

The depositional lobe study could have benefited from a multi methods approach. Within the DEM's alone it is unclear the variation of the areal extent of the depositional lobe and the actual levels of deposition occurring in this area. TLS can provide highly accurate DEM's, but there are limitations in this data collection technique. Given that the Leica C-10 is a single return laser shooting obliquely; it is difficult to obtain true ground returns in areas of dense vegetation without adding several more scanning positions for only limited returns. Other traditional surveying techniques could be used in conjunction with TLS to provide calibration to the results capture via TLS. RTK GPS monitoring of the extent of the rim that can be accurately observed

while in the field. Setting erosion pins in the highly vegetated areas would also provide estimates of deposition occurring in densely vegetated locations and determine a threshold for TLS monitoring in these areas.

While our monitoring capabilities were limited by vegetation it appears that there is extensive deposition occurring on the depositional lobes. Deposited sediment can also be reworked on the lobe due to localized areas of erosion which can transfer sediment to different locations. This can account for deposition without any further input of sediment. Deposition on the lobe was increased greatly during the second year of the study and was comparable to erosion seen within the blowout. While the full extent of the lobe was not captured during the first annual time series, it displayed higher levels of erosion in the lee of the crest. During the seasonal study the summer months had the most deposition. This is surprising given that little erosion was recorded within the blowout. It is possible that fine grain back dune deposits became remobilized in relation to southwesterly winds and were re-deposited on the depositional lobes. It is also possible that intense artifacts in the DEM could have overestimated deposition occurring on the fringe of densely vegetated areas. It is also possible that the increased vegetation in the summer months increased the efficiency of trapping sediment in these areas. During the fall and winter seasons deposition was recorded that was contingent on erosion events occurring within the blowout. Also widespread erosion of the depositional lobe surface is recorded because of the lack of vegetation and the high magnitude wind events in the fall and winter months.

Sub Landform Geomorphology

While sub-landform features have been identified in previous geomorphic studies, they have not been classified and analyzed as separate units. Evans (2012) described increases in

LIDAR capability allowing for the creation of high resolution DEMs in which micro-topographic variation can be used to extract features at the sub landform scale based on variables such as slope and curvature. This level of spatial detail begins to look at the variability through time of different surfaces within the larger scale feature. This classification of a trough blowout is preliminary but patterns do emerge to give more quantitative results on overall trends being observed at the field site.

The transport ramp and lateral slopes consistently were the most active zones during our study. However, on a per unit area basis, the transport ramp and scarp zones demonstrate the highest levels of erosion. The deflation and shelf zones vary between erosional and depositional surfaces. This suggests that they act as temporary sediment sinks in which avalanching from the scarp zones and lateral walls settle in these areas and subsequently removed during following wind events. The deflation basin is appearing to become more stabilized as it approaches the water table and this is supported within our sub-landform results.

Sediment Drift Analysis

Localized topographic steering and acceleration within a blowout make regional wind records inadequate in predicting areas of sediment movement within the blowout; however, the overall sediment drift could be a resultant of the net orientation of multi directional winds (Hesp and Hyde, 1996). Furthermore, correlations have been found between directionality and magnitude of winds recorded at a regional weather station to the geomorphic development of blowouts (Hugenholtz and Wolfe, 2006). Hugenholtz and Wolfe (2006) determined regional winds within an arc of 180 to 330° had the potential for transport but recordings on site did show variations between regional and local wind flow measurements. The Sediment Drift Potential

model allows for the classification of competent events, which provides an understanding of the directionality of these larger events. Topographic steering then becomes evident given the actual trends of erosion taking place within the blowout because it maintains an axis normal directionality regardless of the patterns of major wind events. For instance, the RDP for the three time periods is between 99 and 228°, while the grand mean for erosion only shifts between 127 and 142° during the same time period. This suggests that the influence of multi directional regional wind events become funneled into an axis parallel flow leading to the highest magnitude of erosion occurring along this axis as it approaches the crest of the rim. Deposition was much more variable during these time periods. The grand mean of deposition was recorded between 10 and 332° and were overall lower magnitude in terms of total depositional change. This variability in deposition was observed in the global measurements and appears to be much more contingent on significant individual geomorphic and wind events.

The DP's calculated for the study site in all time periods would all classify this area as a low energy environment. Fryberger's DP values were qualitative representation of sediment drift. He did theorize a relationship between DP and rate of sand drift in m^3/m (width) per year (Fryberger and Dean, 1979). This representation proves to be incorrect given the units used in Fryberger's model were knots, and according to Bullard (1997) this relationship is only valid when using m/s unless you correct the sediment drift equation. When converting the DP's in m/s the max DP value was recorded during the fall season with a value of 0.71. The time period is classified as a low energy environment falling well below the modified threshold of DP<27 (Bullard, 1997). Both the original sediment drift potential and the modified DP values predict negligible amounts of sediment drift per year. However, these predictions were greatly exceeded even during relatively short periods of time.

While using the Fryberger Model (1979) cannot predict airflow characteristics on-site, it does provide an understanding on the level of local topographic steering and acceleration at the study blowout. Hesp and Pringle (2001) found that winds from a 200° arc around the primary axis were funneled into the blowout. This level of topographic steering can be observed from the regional scale as storm events from various directions become steered into the blowout causing erosion continually through the primary axis. Erosion and deposition measurements indicate a high-energy environment, which can only be attributed to the topographic acceleration of air flow in order to have winds that are capable of maintaining sediment transport.

Conclusion

Large-scale geomorphic changes were observed on the annual temporal scale. Mass expansion was observed during the first year during the capture of an embryo dune. The second year showed less change as the feature elongated up wind and downwind along its axis and is probably more representative of annual expansion taking place at the study site. Volumetric changes remained at a high level during both years of the study. The deepening of the blowout appears to intensify the levels of erosion along the axis; however, the deflation basin is already beginning to approach the water table and may become stabilized from the increased surface moisture. Changes in the blowout are driven by storm events that occur in the fall and winter months. The cyclical evolution, hypothesized by Gares and Nordstrom (1995), is not reflected in the time frame of our current study. The results do not provide evidence that stabilization is the next stage in the evolutionary process of this feature.

Sub landform classification of geomorphic zones within blowouts has the potential to provide more understanding of net changes and the rate of change that is experienced between

the different zones. The systematic classification and the quantification of changes that are taking place in these zones moves beyond the empirical observations that have been used to describe changes taking places in these loosely defined areas. The transport ramp and the lateral slopes experience the largest volumetric flux of sediment, however, normalizing these zones per unit area the transport ramp and the scarp zones are consistently the most highly active surfaces within the blowout. The deflation basin appears to become stabilized during the second year of the survey evident by the net volumetric changes of high levels of erosion shifting to a surface that only experiences slight erosion. The results may be result of unique characteristics at the study site and the classifications of other blowouts will provide a broader understanding of blowout geomorphology.

The greatest geomorphologic changes occur during storm events that become magnified by unique topography of the study blowout. While seasonality corresponds with these changes, (i.e. more storminess occurs during the winter) storm events at any period will lead to large-scale geomorphic changes within the trough blowout. Even winds with an oblique approach to the primary axis can be steered into the blowout leading to major volumetric changes within the blowout. This can be shown by the comparison of the directionality of wind events via the Sediment Drift Potential model and the subsequent erosion centered on the axis of the blowout, which remains relatively constant. During the winter month there is the greatest activity of Nor'easters and other storm events, which lead to the majority of changes occurring during this time period while little changes occur during the summer when winds are of low magnitude and non-axis normal. Other seasonal factors such as solar aspect, temperature, and solar radiation appear to have little impact on the large-scale evolution of the blowout. Seasonality differences

are observed, but the driving forces for the large-scale geomorphic changes observed at the blowout are high magnitude wind events.

Chapter 3: Geomorphic Impact on Development and Capture of Embryo Dune Blowouts, Cape Cod National Seashore, MA

Introduction

Blowouts are common erosional features that develop in dune landscapes and that generally exist in either trough or saucer shapes (Hesp, 2002). These landforms have been observed in a wide variety of environments and regions including northern Europe (Jungerius et al., 1981; Den Van Ancker et al., 1985; Jungerius and Van der Meulen, 1989; Jungerius et al. 1991; Pluis, 1992; Neal and Roberts, 2001; Kayhko, 2007; Smyth et al. 2012), North America (Gares, 1992; Gares and Nordstrom, 1995; Fraser et al., 1998; Anderson and Walker, 2006; Hugenholtz and Wolfe, 2006; Hansen et al, 2008; Hugenholtz and Wolfe, 2009; Hesp and Walker, 2012), Australia and New Zealand (Hesp, 1996; Hesp and Hyde, 1996; Hesp and Pringle, 2001), and South Africa (Bate and Ferguson, 1996). Although blowouts are often generated from aeolian processes, their development may be enhanced by a number of controlling factors. In coastal foredune systems, blowout development may be facilitated by wave erosion along the dune face that narrows the dune ridge in places, making it more susceptible to wind scouring. Reduction of vegetation density in sections of a dune system due to short-term drought, longer-term climate change, competition from other dune vegetation species or pest infestation also may result in dune erosion and eventual blowout formation. Blowout formation is often also linked with human activities that result in vegetation loss and displacement of sand particles (Hesp and Hyde, 1996; Hesp, 2002). Despite this assumption regarding the effect of human activities on blowout formation, their existence in natural systems suggests they are a normal component of complex dune landscapes. Previous studies provide evidence for trough blowouts forming on the stoss face of dune ridges, while saucer blowouts

develop on elevated dune ridges (Smith, 1960; Jungerius and Van der Muelen, 1989; Hesp, 2002). However, there are few geomorphic studies that document where these incipient blowouts form and how they evolve from initiation. Studies have examined long-term evolution of blowouts (Jungerius and van der Muelen, 1989; Gares, 1992; Gares and Nordstrom, 1995; Hugenholtz and Wolfe, 2006; Kayhko, 2007), but there is limited information about the morphodynamics of blowouts in the early stages of their development. The aim of this research is to study these feature in terms of their initiation, development, and interaction with the adjacent area in which they form.

This research is a continuation of a larger study on blowouts taking place at Cape Cod National Seashore. This has led to the first description of the significant geomorphic evolution of small scale embryo blowouts and their role in the larger blowout environment (Smith et al., 2013). Embryo blowouts are incipient dune blowouts that form in sheltered or nested areas of the landward side of exposed dune ridge (Fig. 19). These features have been observed to form within a few meters of the crest of their host blowout or dune ridge. The difference between embryo blowouts and other incipient blowouts is that these features have the potential to be captured by the host feature through ridge collapse and subsequent landform coalescence. There is a significant geomorphic impact on the host feature, from both an initial response and legacy of short-term evolution (Smith, 2013). A ridge separating the embryo blowout and the host blowout failed and led to mass expansion of the original landform. In subsequent years, sediment transport was enhanced by the increased connectivity associated with the embryo capture. Smith et al. (*2013*) provide a new consideration of blowout development by providing a detailed account of embryonic dune capture by its host blowout. Embryonic dune capture provides a new understanding on the ways in which blowouts expand overtime. While Smith et al. (*2013)*

describe these features as ubiquitous across Provincelands dunes in Cape Cod, MA; the role of these features in other dune blowout environments is unknown. We have, however, observed similar features in the dune field at Sandy Neck, on the north shore of lower Cape Cod. Provincelands dunes provide a great natural laboratory in which the geomorphic significance of these features can be studied.

Figure 19: Embryo blowout in Provincelands dune field on Cape Cod, Massachusetts. The Atlantic Ocean is just over the foredune ridge visible on the left side of the photograph; dominant winds are northerly also to the left.

Previous geomorphic studies on blowouts have quantified the changes in morphometry of dune blowouts through time (Jungerius and van der Meulen; Gares, 1992; Hugenholtz and Wolfe, 2006; and Kayhko, 2007). Also empirical models and observations have been used to describe blowouts as cyclical (Gares and Nordstrom, 1995), or at least have proposed a critical size of these features due to airflow and sedimentological limitations (Gares and Nordstrom, 1995; Hesp, 2002; Hugenholtz and Wolfe, 2006; and Hesp and Walker, 2012). Missing from the larger literature is the role of embryo dunes in the rapid geomorphic modification of the host

blowout. The role of embryo blowouts must be considered when addressing the larger evolutionary tracks of blowouts. Increasing our knowledge on both embryo dune blowouts and their host blowout will provide new considerations on where these features are forming and the geomorphic significance of embryo dune capture. This study monitors the development through time of embryo dunes by analyzing aerial photographs and conducting high resolution topographic surveys. Focusing on the evolution of these features both prior to and following capture will provide insight in the initiation and expansion of these features as well as the larger geomorphic implications embryos have on the host feature.

Lee Side Morphodynamics

The lee of dune blowouts has often been described as an area of accretion, causing the creation of depositional lobes that are formed downwind of the crest. As airflow compression and acceleration occurs through the blowout axis it reaches maxima velocity at the crest followed by a subsequent expansion and deceleration occurring in the lee (Hesp and Hyde, 1996). The depositional lobe, however, can be very dynamic and can experience high levels of both deposition and erosion (Smith et al., 2013). Secondary wind patterns have the potential to redistribute sediment across the lee slope. Nickling et al. (2002) found that up to 99% of deposition occurred within two meters of the rim of a transverse dune, but it was also observed that vertical uplift and turbulence present in the wake had the potential to move sediment. Walker and Nickling (2002) provided a detailed description of the role of secondary airflow on sediment transport and the debate in the larger literature of the geomorphic implications. Wind tunnel studies have shown the area of detachment can form reversed flow and can generate shear stress of up to 40% of the maximum (i.e. at the crest). The greater geomorphic significance remains in question but both recorded and modeled results have shown that reversed flow has the

potential to transport sediment back towards the lee slope as well as laterally along the slope (Walker, 1999; Walker and Nickling; 2003). While studies looking at this phenomena have been widely conducted in the larger dune literature it is unknown the impact that this secondary airflow has on the initiation and expansion of embryo blowout dunes.

Study Site

This study was conducted at Provincelands dunes, which is part of Cape Cod National Seashore (Fig. 20(B)). The dune field is located at the northern extremity of Cape Cod, Massachusetts, a complex recurved spit that was created during the period of sea level rise that followed the most recent glaciation, when glacial deposits were reworked by ocean processes starting around 18,000 bp and developed into the coastline that exists today. The wave regime produces dominant alongshore transport to the north, and the sediment thus transported was deposited at the distal end of the spit (Smith et al, 2004). This Holocene dune field consists of inland parabolic dunes and a coastal transverse dune system (Formen et al., 2008). These coast parallel transverse dune ridges and trailing arms of the parabolic dunes are characterized by slipfaces that face to the southeast to southwest. These characteristics suggest the dominance of competent winds occurring largely from the northerly directions (Fig. (A)). The inland dunes were created during periods of low vegetation cover that allowed for a highly dynamic dune field (Smith et al. 2004). English settlement in the late 17th century reactivated Provincelands dunes by deforesting the area (Forman et al., 2008). The removal of forest cover has exposed a large amount of sediment to aeolian forces and this area has remained highly dynamic.

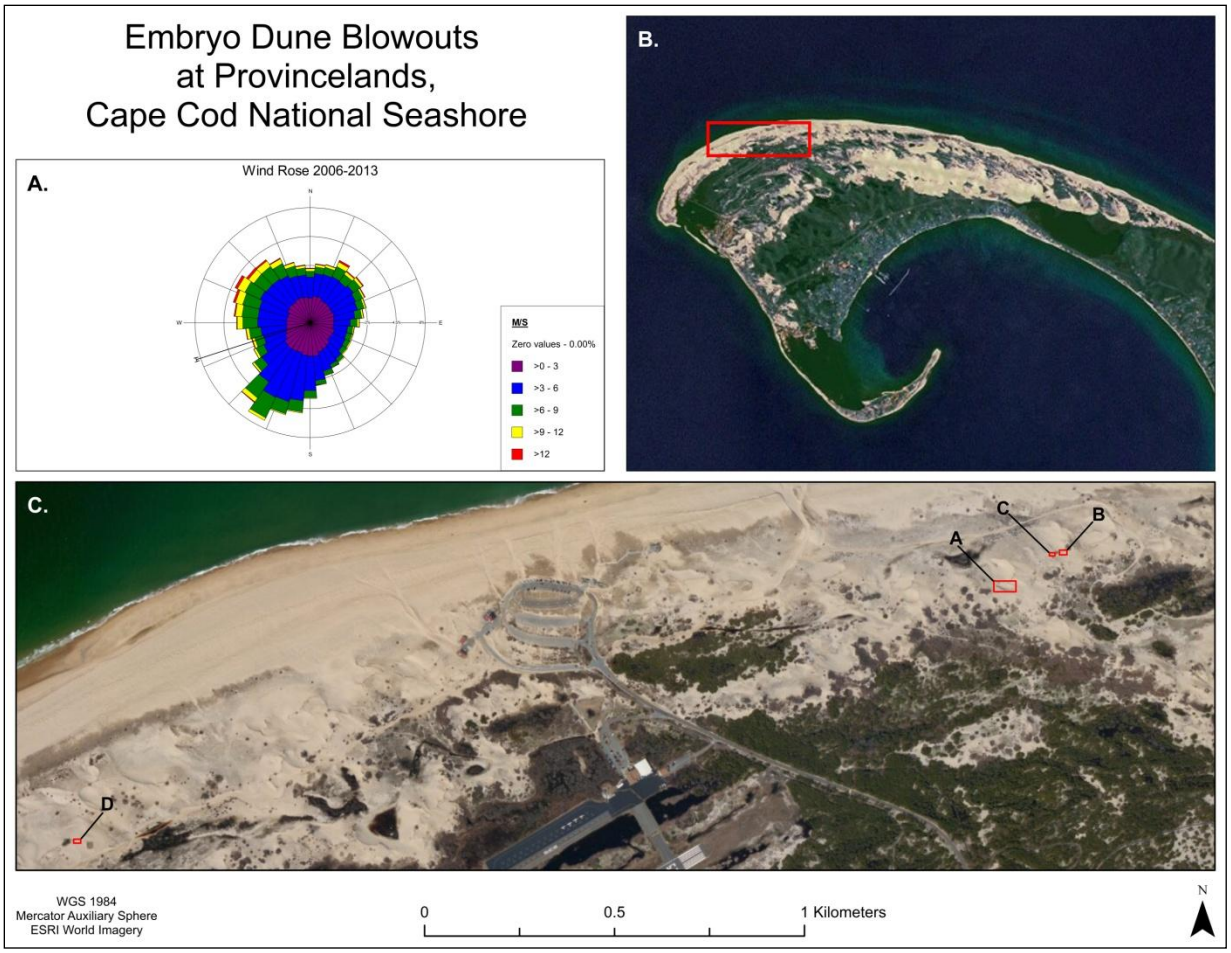

Figure 20: Province Lands Dunes, Cape Cod National Seashore. Embryo blowouts develop in the lee of exposed blowout and dune ridges.

Embryo blowouts are common features at Provincelands dunes that develop in the inland crest of larger host blowouts as well as exposed dune ridges. High magnitude northerly winds (Fig. (A)) erode into the shore parallel transverse dune ridges and the trailing arms of the parabolic dunes. These locations are often where trough blowouts form with a primary axis usually oriented to these northerly winds. Embryo blowouts then form within a few meters inland from the crest of these trough blowouts or other gently curving dune ridges. Blowouts at Provincelands are sensitive to seasonal variations in weather and vegetation cover. During the

fall and winter months high magnitude northerly winds occur more regularly. This coincides with reduced vegetation cover (i.e. American Beach Grass) and leads to a highly dynamic dune field during the late fall to early spring (Smith et al. 2013). This study will focus on four embryo blowouts that are located within ~2.7 km of each other (Fig. 20 (C)). Embryos A, B, C, and D were all topographically surveyed at varying intervals between May 2011 and May 2013.

Methodology

Data Collection and Processing

Geomorphic change detection is captured through repeat topographic scan surveys using Terrestrial Laser Scanning (TLS) (Wasklewicz and Hattanji, 2009). TLS surveys are collected using a Leica C-10 Laser Scanner. The Leica C-10 is single return laser so multiple scan positions are needed in order to capture the entire surface of the embryo blowout. These features are relatively small in scale and an average of 2-3 scans are needed to capture the surface and to fill in the data voids as a result of shadowing. More scan positions are also added in order to capture the topography adjacent to the blowouts. Multiple scan positions are integrated into one three-dimensional point cloud using a series of Leica HDS planar targets. Leica HDS targets are geo-referenced using a Trimble RTK GPS unit, which allows for the repeatability of surveys as well as providing a common coordinate system in which changes can be monitored through time.

Propagated error budgets are created for each embryo location. The Root Mean Square Error (RMSE) and Standard Deviational Error (σ) are commonly used error measurements that were calculated (Staley et al., 2011; Staley et al., *under review*). These values provide a conservative level of error associated with both user and systematic error during the TLS scan surveys. Error measurements provide global error values that can be assigned to individual pixels

across the entirety of the Digital Elevation Model (DEM). A +/- value can also be derived for each volumetric measurement. Error for all scan surveys are ≤ 1cm providing a low level of error that will allow for the quantification of small scale topographic changes within the DEMs (Table 6)

Study Site	RMSE	σ error
Embryo A	8.3 mm	8.5 mm
Embryos B and C	10.59 mm	10.34 mm
Embryo D	7.87 mm	7.88 mm

Table 6: Location and error associated with each TLS survey.

The LiDAR filtering software LAStools was used in order to generate bare earth models that allow for accurate geomorphic measurements to be made. The presence of vegetation in the LiDAR point clouds could over or under estimate topographic changes occurring between subsequent scan surveys. User defined code sequences removes points above the estimated ground surface. Any residual artifacts were removed by thinning the data. Data thinning also provides consistent point spacing across the entirety of the surface which reduces the potential for large spatial error during the DEM generation. Once vegetation was removed a 10x10 cm DEM was generated in ArcMap for all four of the embryos.

Geomorphological Mapping

Repeat TLS surveys permit monitoring of the areal extent and the volumetric changes of the embryo dune blowouts through time. DEMs are created along with other mapped surfaces (i.e. hillshade and curvature) and permit identification of the areal extent of these features. Visible breaks in slope representing a crest is used to delineate the boundaries of the landform. These boundaries are digitized in ArcGIS and the expansion and contraction of these

rim polygons are monitored throughout all scan surveys. The dynamic evolution of the rim provide an understanding on the morphometrics of the embryo blowouts during our study.

The DEMs are differenced to capture the surface elevation changes from each survey in the multi-year surveying campaign. Volumetric changes at the study site are produced from 10x10 cm pixel planimetric resolution and converted to m^3 values. Changes in elevation within each 10x10 cm pixel are converted to volumetric measure per each cell. Each scan survey are differenced from the previous survey allowing for these elevation and volumetric measurements to be made from subsequent scan surveys. The corresponding rim polygon for each survey will be used as the boundary in which the volumetric measurements will be made for each embryo blowout. These topographic surveys and geomorphic measurements allow for the creation of highly detailed sediment budges monitoring the flux of sediment within each study embryo.

Historical Development

Aerial photographs provide a time-frame in which initiation occurs because they allow for identification if not the measurement of the recently initiated features. Visible defomations on the inland slip-face of dune ridges help identify previously recorded embryo blowout, allowing for a historical timeframe that these features developed. Aerial photographs also allow for the delineation of previously recorded embryos and provide a quantifiable areal extent of the landform in ArcGIS. The historical initiation and expansion of the embryo dunes were monitored using a series of ortho-rectified aerial photographs that were collected from the USGS and USDA. Aerial photographs were available for nine years since 1990, however, only the photographs from 2009 were of adequate quality in order to make accurate areal measurements. The spatial resolution and quality of these aerial photos range widely due to both pixel size and

exposure of the photographs. In most cases, these aerial photographs cannot adequately define the entire boundary of the incipient embryo blowouts but can provide an estimated time period that these features originally became initiated.

Results

Embryo A

During a ground reconnaissance in April, 2008 at the large trough blowout, a small incipient embryo blowout was found just inland of the blowout crest (Figure 21). Inspection of aerial photography reveals that a second embryo saucer formed adjacent to the first one in May 2009, totaling an area of 40.39 m^2 (Fig. 22). By the spring of 2011, the two small embryo blowouts had coalesced into one and the overall area covered by the embryo was 408.7 m^3. Although they were separated from the main blowout by ~3 meters at initiation, the ridge between them had narrowed considerably by 2011. Embryo A had grown from a small-scale incipient blowout to a large embryo saucer blowout in roughly a three-year period and was on the brink of capture from its host blowout.

Figure 21: Trough blowout in April 2008 with embryo A shown in inset and its location on the blowout crest indicated with the arrow.

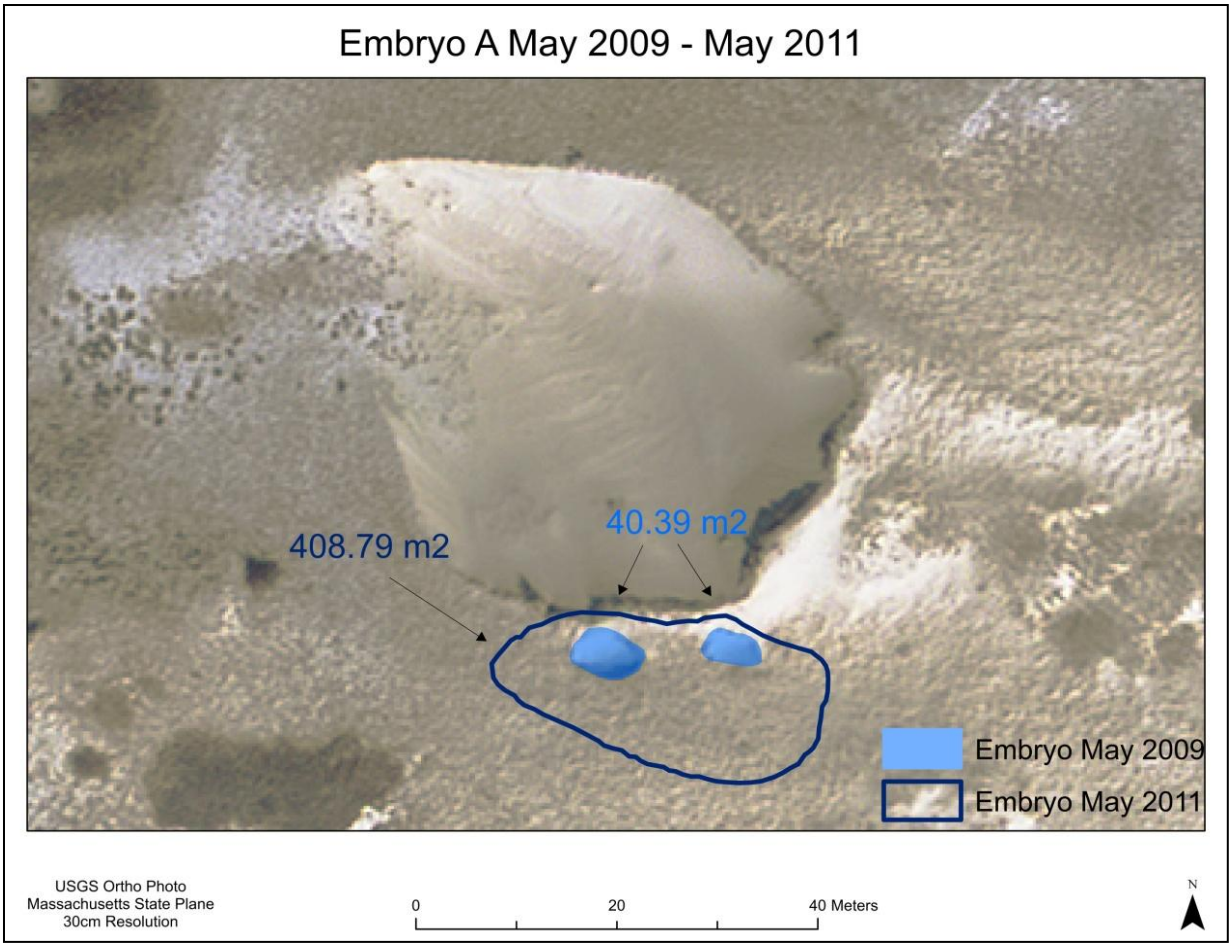

Figure 22: Expansion of Embryo A from two small incipient blowouts to one large embryo blowout from May 2009 – May 2011.

Our initial TLS survey was conducted in May 2011 which was followed by a subsequent survey in May 2012. Prior to the second survey the embryo blowout was captured by its host blowout providing a detailed understanding of this process. The failure of the ridge that separated the two features, involved the removal of 238.41 m^3 of sand, while the deflation basin of the embryo filled with 171.95 m^3 of sand (figure 23). While this provides only an initial response to the embryo blowout capture, the capture embryo blowout greatly modifies the geomorphology within the larger host blowout. As the embryo and its host morphed into one

larger feature, the ramp from the floor of the host blowout to its ridge extended through the former embryo (Fig. 24). Expected streamline acceleration of airflow through this newly exposed feature rapidly eroded the lateral wall and scarp areas of the former embryo following capture leading to a 111.26 m^3 of erosion in these areas (Fig. 23).

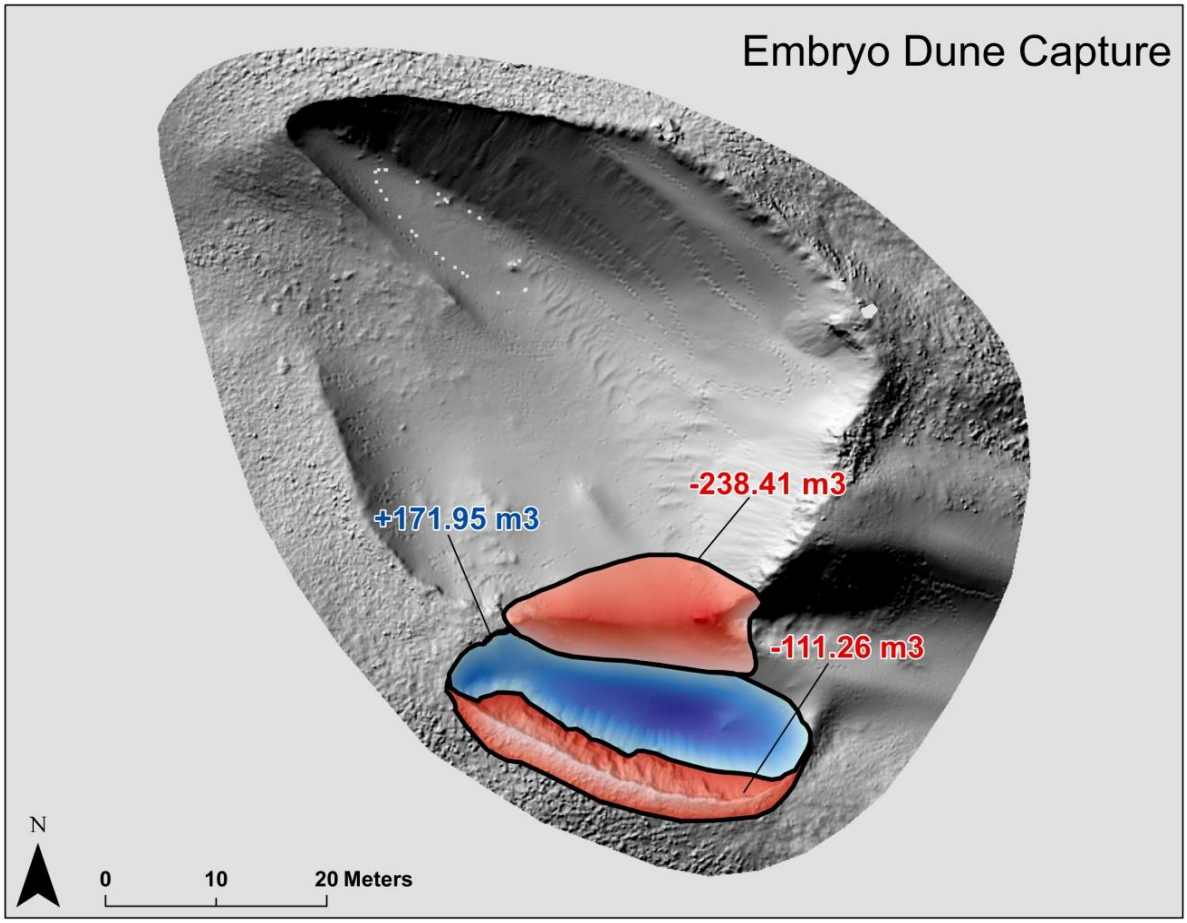

Figure 23: Initial geomorphic response due to the ridge collapse separating Embryo A and its host dune blowout.

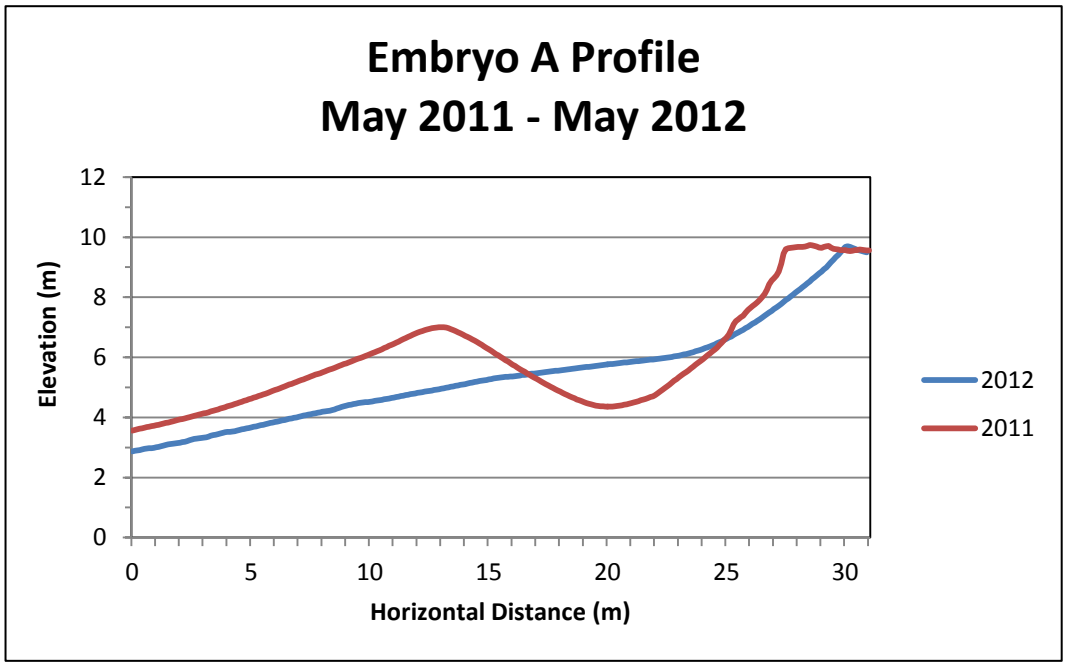

Figure 24: Profile extending through the axis of the host blowout and across the embryo blowout before and after capture.

Embryos B and C

Two small embryo blowouts were identified to the east of blowout complex A, and these were also surveyed in May 2011. Embryos B and C were absent from the aerial photographs prior to the May 2011 survey, however, the May 2010 photographs quality wouldn't allow for small scale features (i.e. incipient embryos) to be visible. The two embryos likely developed in the winter of 2010 or 2011. The initial survey conducted showed that blowout B was larger and more developed suggesting it was initiated first. Embryo C was small and likely was more recently initiated prior to the original TLS survey.

In May 2011 embryo B was 55.58 m², while embryo C was 12.17 m² (Fig. 25). The following year (i.e. May 2012) embryo B recorded modest expansion to 61.52 m² (Fig. 25). During this time embryo C more than doubled in size to an areal extent of 25.48 m² (Fig. 25).

Both embryos displayed growth downwind of the crest and lateral expansion (i.e. East to West). The upwind extent of these features closest to the crest remained relatively static. The second year, following a survey in May 2013, displayed significant expansion of both embryo blowouts. Blowout B grew to 120.99 m² and embryo C grew to 47.34 m² (Fig. 25). Embryo B once again showed significant expansion both downwind and laterally. During this time period embryo C expanded in both up and downwind directions as well as displaying growth laterally. The ridge separating embryo C and the adjacent trough blowout has become significantly diminished; indicating capture of this embryo is imminent during the next winter storm season.

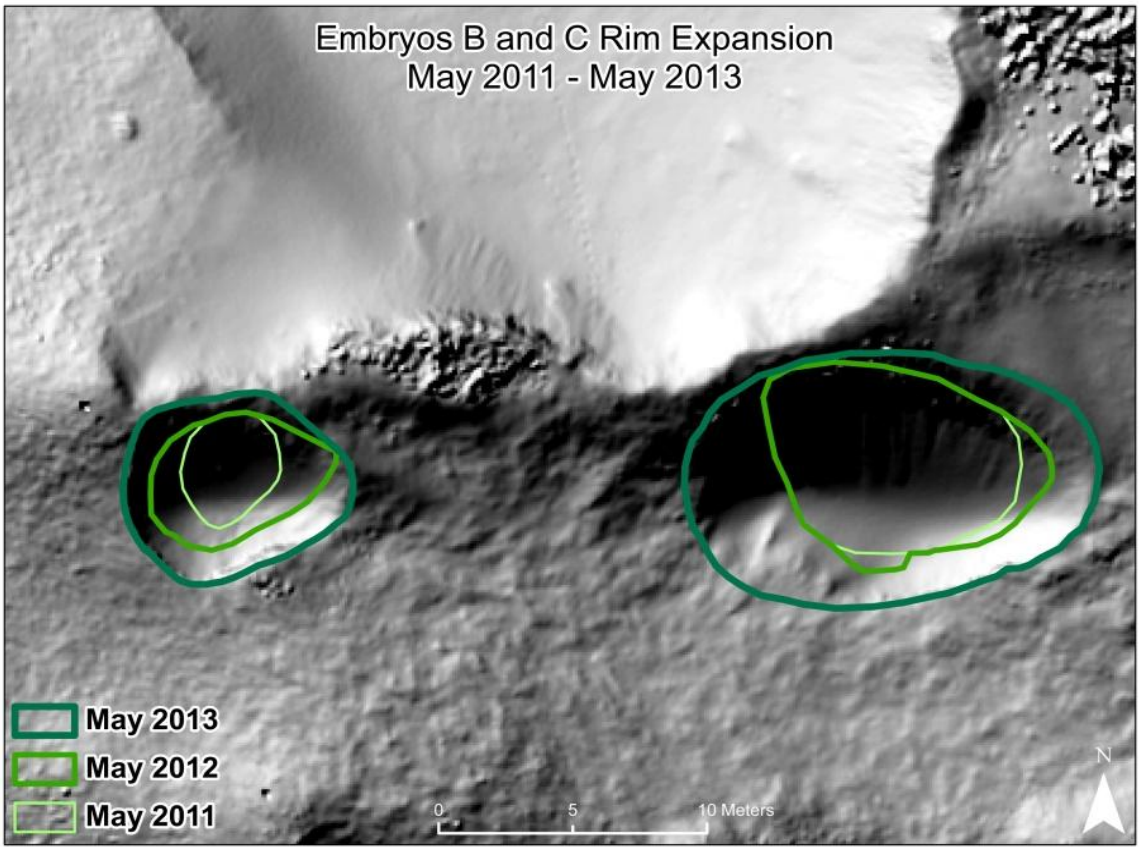

Figure 25: Rim polygons showing the areal extent of Embryos B (right) and C (left) between May 2011 and May 2013.

Embryos B and C are small-scale incipient blowouts and they a largely erosional surface (Fig. 26). During the first year of the study embryo B had a net of 12.56 m^3 ± 0.65 m^3 of erosion (Table 1). Embryo B had the most pronounced erosion on the southwestern section of the blowout downwind from the crest. During this time period embryo C had a net of 5.88 m^3 ± 0.29 m^3 of erosion (Table 7). Embryo C experienced the most erosion on the Southwestern section of the blowout downwind from the crest. In year two of the study, embryo B had a net of 45.42 m^3 ± 1.28 m^3 of erosion (Table 7). Embryo C had a net of 16.71 m^3 ± 0.50 m^3 of erosion during this time period (Table 7). Embryo B experiences the highest levels of erosion on the Southeastern section of the blowout while embryo C has the highest levels of erosion on the southwestern section of the blowout. Overall erosion tends to be dominated on the inland of the embryos and deposition occurring in the northern sections particularly in the northeast suggesting a possible detachment over the crest and recirculation of high magnitude northerly winds.

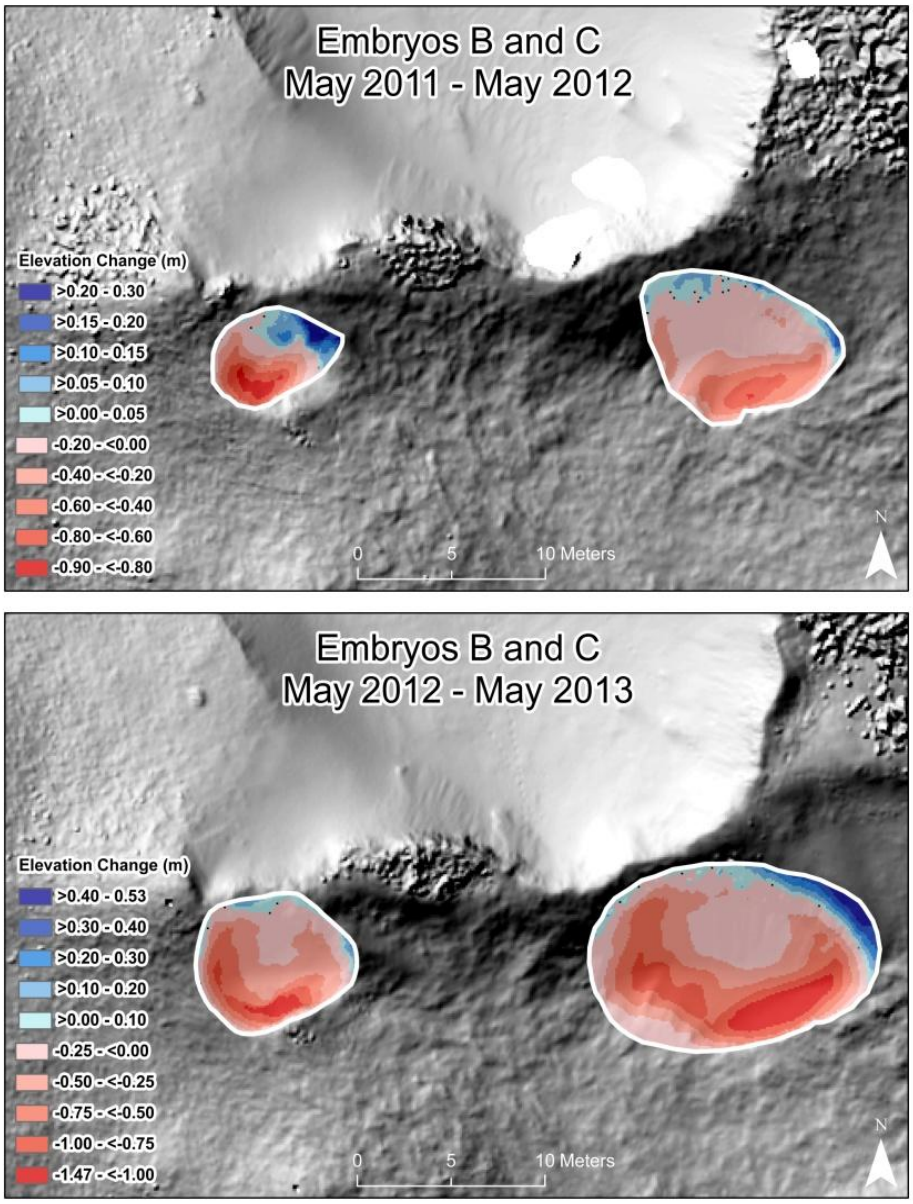

Figure 26: Difference of surface rasters showing topographic changes occurring at Embryos B (right) and C (left) between May 2011 and May 2013.

	Embryo B				Embryo C			
	Area m^2	Erosion m^3	Deposition m^3	Net Change m^3	Area m^2	Erosion m^3	Deposition m^3	Net Change m^3
May-2011	55.58	N/A	N/A	N/A	12.17	N/A	N/A	N/A
May-2012	61.52	-12.99 ± 0.56	0.43 ± 0.10	-12.56 ± 0.65	25.48	-6.68 ± 0.18	0.79 ± 0.09	-5.88 ± 0.27
May-2013	120.99	-48.23 ± 1.12	2.80 ± 0.16	-45.42 ± 1.28	47.34	-17.03 ± 0.45	0.32 ± 0.05	-16.71 ± 0.50

Table 7: Area and Volumetric measurements recorded at Embryos B and C between May 2011 and May 2013.

Embryo D

Embryo D is a saucer blowout located ~1.9 km West Southwest of embryo A (Fig. 20). Embryo D has formed just in the lee of the crest of an exposed linear dune ridge. This embryo was first identified in the aerial photograph records in 2012 and likely formed between the winters of 2011 and 2012. Embryo D is unlike the other embryo dunes because it hasn't formed adjacent to a host blowout, however, the curvature of the ridge is analogous making the development of these features comparable. While only two TLS surveys were conducted at this site, embryo D was captured by its host (i.e. ridge failure between the embryo and host feature), providing another example of embryonic dune capture at Provincelands Dunes. During our initial TLS survey of this site in October 2012, embryo D totaled 39.40 m^2. During our following survey in May 2013, the embryo had grown to an aerial extent of 73.03 m^2 following capture, almost doubling its former size (Fig. 27).

Following a highly active winter storm season the embryo had been captured after the ridge collapse. Embryo D had a largely erosional surface with a net of 39.88 m^3 ± 0.57 m^3 of

erosion. After the ridge failed there still remains a slight lip prior to entering the blowout (fig. 28). But the bowl itself appears to have shifted downwind and it recorded extensive erosion of the southern lateral wall. While this provides another snapshot of the initial response to embryo dune capture it could provide a better understanding on blowout evolution because it is not an extension of a previously developed blowout and it remains unclear how this feature will continually evolve.

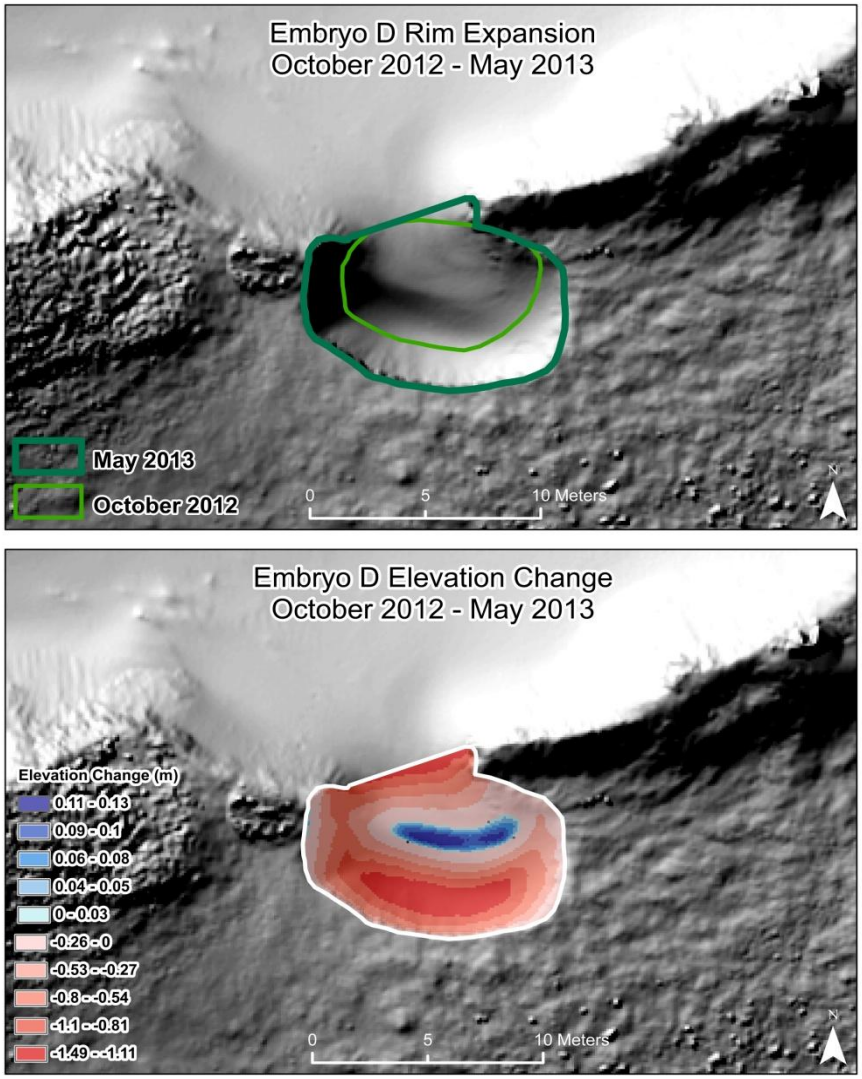

Figure 27: Areal extent and topographic changes occurring at Embryo D between October 2012 and May 2013.

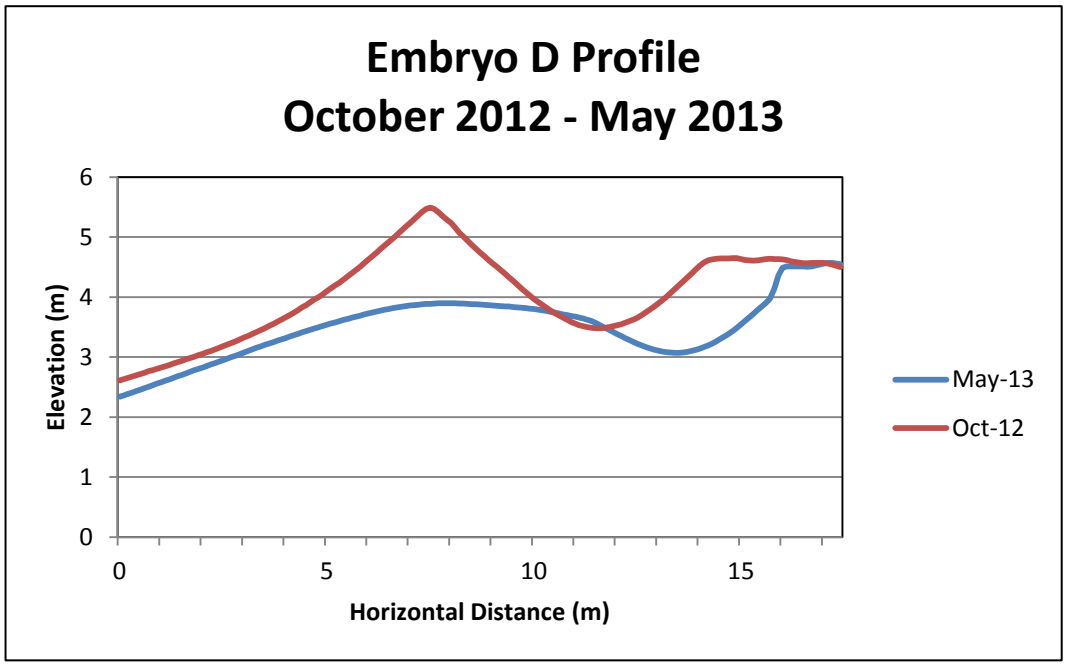

Figure 28: Profile extending across the host feature ridge and over the embryo blowout before and after capture

Discussion

Initiation and Expansion

The initiation of incipient blowouts has been addressed in the larger blowout literature (Hesp and Hyde, 1996; and Hesp, 2002), but the detailed geomorphic examination of these features has been lacking. The ability to map these features becomes an issue due to their small spatial scale and their rapid expansion. This study has been able to capture the rapid expansion of embryo dunes through high resolution topographic TLS surveys. Limitations in the quality of aerial photos has limited the ability in most cases to monitor these features progressively through time. This has limited the number of embryos that could be adequately monitored through time, however, the TLS data collected has provided detailed morphometrics and sediment budgets of these incipient blowouts. The morphodynamics of both embryos and other incipient embryos

must be studied further with the implementation of high resolution geomorphic mapping techniques.

Studies of airflow in blowouts (Hesp and Hyde, 1996) show the highest wind speeds occur along the primary axis. Flow compression and acceleration, and our analysis (Smith et al., 2013) of topographic change in the host blowout show the highest erosion occurs along the same axis. In addition, embryo A formed in the lee of the crest in line with the primary axis. The other blowouts appear to have formed in similar locations. The locations of embryos B and C suggest they have also developed parallel to axis of the host feature in which topographic acceleration of airflow is expected. The divergence of two discrete trough features is visible with the trough adjacent to embryo B oriented Northwest to Southeast, and the trough adjacent to embryo C oriented Northeast to Southwest (Fig. 29). The orientation of these trough features is significant because as winds become accelerated parallel to the axis you would expect higher magnitude winds and greater development of secondary airflow in the lee of the crest.

The area inland of the blowout crest is a highly depositional surface particularly in the northeastern area adjacent to the blowouts (Fig. 29). Maximum erosion occurs within the blowout downwind of the crest and laterally (i.e. East to West) along the lee slope. Intuitively you would expect max erosion to occur downwind of the incident wind angle. The upwind section (i.e. towards the crest) remains relatively stable in comparison. These observations lend themselves well to the recorded measurements both in the field and in wind tunnels of secondary airflow patterns in which both transverse and slightly oblique winds over the crest can potentially reverse flow both up the lee slope as well as laterally across the lee slope (Walker, 1999; and Walker and Nickling 2002). This was further supported by surveys conducted following the summer and early fall months in which embryo B and C recorded little geomorphic change.

These time periods have incident wind angles mainly coming from the southwest and are of relatively low magnitude. This flow up the lee slope appears to have little geomorphic impact on embryos B and C and most of the changes occurred during the winter months when strong northeast and northwest winds impacted the study site. The role of secondary airflow appears to be significant as the longitudinal axes of these features are expanding perpendicular to the incident angle of competent airflow events.

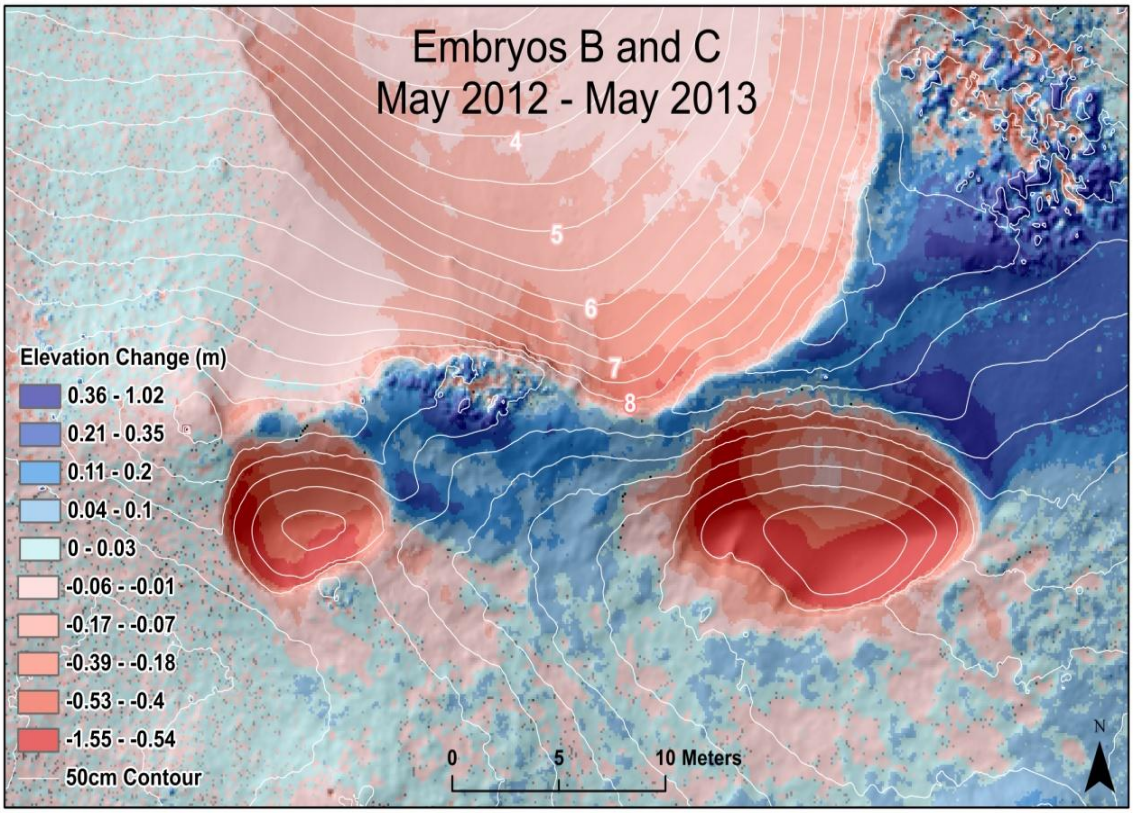

Figure 29: Embryos B and C following TLS survey in May 2013; showing patterns of depositions and erosion.

Geomorphic change detection monitoring of these features suggests an approximate doubling in size each year. This expected growth of the blowouts was not achieved by embryo B

in the surveys between May 2011 and May 2012. During this time period embryo B experienced relatively high levels of erosion, but the rim only expanded slightly downwind and laterally on the Eastern section of the blowout. It is unclear if the orientation of high magnitude winds or the persistence of vegetation had a role in the limited growth during this time period, however, in year two of the study embryo B nearly doubled in size which corresponds to the growth we have documented at the other sites during our TLS surveys. Embryo A expanded more rapidly as verified by both field observations and the historical aerial photographs. Embryo A initially developed as two discrete embryos that became one larger scale embryo as the two features grew together. Smith et al. (2013) found embryo A's host blowout experienced intense erosion through the axis of the blowout and amplified topographic acceleration of flow could have led to the hastened levels of expansion of embryo A. Overall, expansion of the embryo blowouts occur rapidly and these features appear to become captured within a period of only a few years following initiation.

Capture and Geomorphic Implications

Two embryo blowout captures have been recorded and the larger geomorphic implications are significant. The rapid development of these features from initiation to capture appears to be occurring on a sub-decadal scale. Capture leads to mass expansion of the host blowout or possibly the initiation of larger scale features (i.e. incipient trough blowouts). For instance in the period between the 2009 aerial photographs and the initial TLS survey in 2011, embryo A's host blowout only expanded by 100 m². This is compared to the growth of the embryo that in the same time period expanded over ten times its original size from 40.39 m² to 408.79 m² (Fig. 22). While the larger collection of aerial photos (i.e. other than 2009) does not provide a consistent year-to-year quantitative history of expansion, qualitatively the expansion of

the larger host trough remains relatively consistent. The growth of this feature appears to be up and downwind along the axis, which corresponds well with previous studies looking at the long-term evolution of dune blowouts through aerial photography (Jungerius and van der Muelen, 1989). However, the rapid growth of the embryo and the subsequent capture of this features led to an expansion of 563 m^3 of the overall blowout area, which led to the growth of the host blowout of over a quarter of its original size (Smith et al., 2013). We know that the initiation of embryo A occurred around 2008 and by 2012 the host blowout had expanded significantly, well beyond the expected normal growth rate. Embryo dune capture has provided a new understanding on the rapid expansion of blowouts occuring in symbiosis with the develepment of adjacent embryo blowouts. Rapid modifications to these landforms appear not to be occuring over decades but a much a much faster rate given the development and capture of embryo dunes.

Embryo D provides a slightly different example of embryo dune capture. Since this embryo did not form on a preexisting blowout it is unclear the long term evolutionary significance of the blowout. Embryo A led to the linear growth of the host blowout parallel to the axis. Embryo D may provide an understanding on how trough blowouts are initiated. It is believed that troughs become initiated as they begin to erode into the stoss slope of an exposed ridge. While this may work well to describe initial deformation of foredunes exposing them to further aeolian erosion (Hesp and Hyde 1996; Hesp, 2002), it is not clear the role of aeolian processes in the initiation of trough blowouts for inland dune fields. It appears the embryo D has the potential to become a larger trough. As of now it is elevated but the base level may drop significantly in the coming years as North and Northeast winds will likely be accelerated through this new breach in the otherwise semi-linear dune ridge.

Following its catpure in May 2013, embryo D had similar patterns of initial geomorphic response in comparison to embryo A (Smith et al., *under review*). Embryo D experienced high levels of erosion in the former ridge area and downwind lateral wall and scarp areas (Fig. 30). Also, deposition was recorded in the initial deflation basin (Fig. 30). After the embryo blowout became captured and erosion was accelerated on the downwind section, it led to a widespread deposition surrounding the embryo. The newly opened area likely funnels and compresses air through the feature causing accelerated airflow and subsequent sediment transport patterns. While the geomorphology of the initial response in both embryo captures was similar, it is unclear the longer term geomorphicevolution of these features..

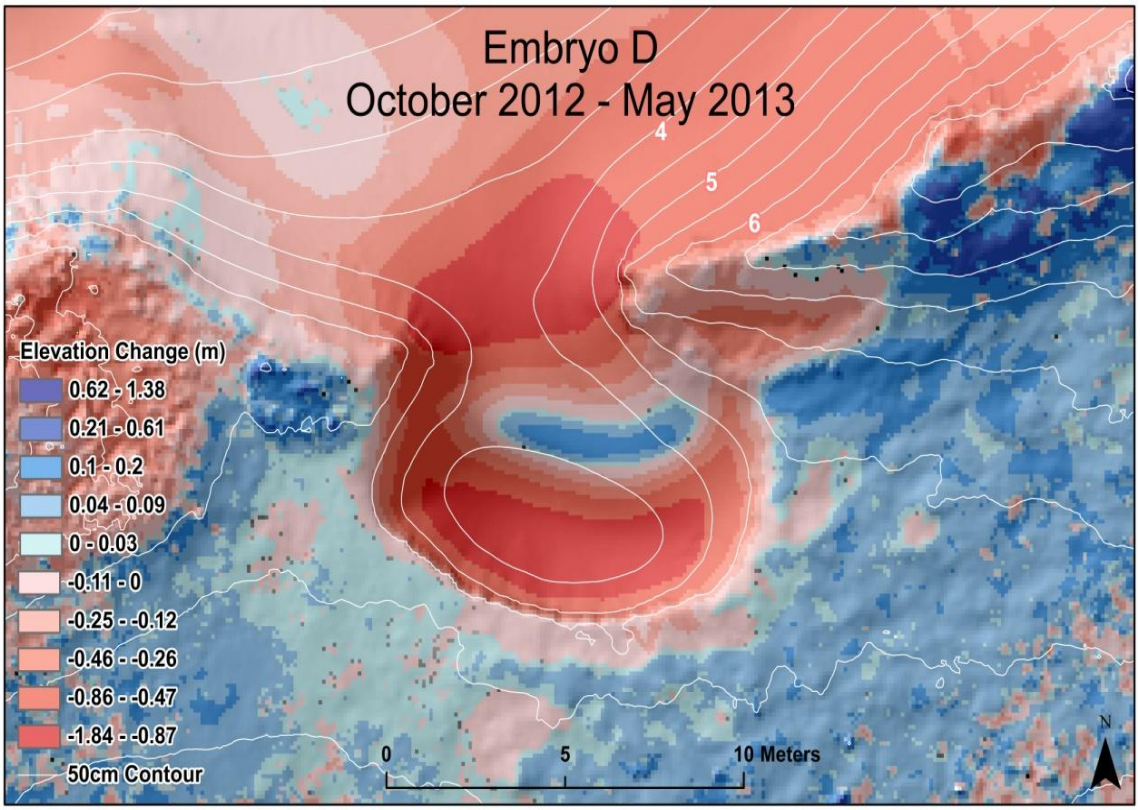

Figure 30: Embryo D following a TLS survey in May 2013; showing patterns of deposition and erosion.

Theoretical Model of Embryo Development

While the current study uses a limited number of embryo blowouts that represent a small portion of Provincelands, our intensive monitoring of these dunes using multiple techniques presents an opportunity to develop an initial theoretical model of blowout growth.

i) Deposition occurs in the elevated lee slopes of blowouts and exposed dune ridges.

ii) Embryos become initiated within a few meters in the lee of the crest due to secondary airflow process (i.e. recirculation of flow in the separation zone) during major wind events.

iii) Embryo blowouts rapidly deflate the unconsolidated depositional sediment in the lee of the crest and roughly double in size each year. Blowout expansion is maintained downwind through back-flow eddies and laterally-flow helical vortices.

iv) Embryo dune capture (i.e. ridge failure between the embryo and its host) occurs on a sub-decadal scale.

v) Rapid erosion occurs in the newly exposed area leading to mass expansion of the host feature and alters subsequent airflow and sediment transport patterns.

Conclusion

Embryo blowouts our observed to initiate on the sheltered lee of elevated dune ridges a few meters downwind of the crest. Following initiation embryos expand rapidly and potentially can become captured by its host feature within only a few years. The upwind (i.e. towards the crest) section of the embryos remains relatively static while the downwind and longitudinal sections experience rapid growth. Capture then takes place as the slope of adjacent ridge

encroaches on the embryo until the there is a breach and the two landforms coalesce into one larger feature. Following capture the area of the former embryo remain highly dynamic. Embryos form parallel to the primary axis of the blowout and airflow is accelerated through the relict structure causing further erosion. This study has focused on both the expansion (i.e. embryos B and C) and the capture (i.e. embryos A and D) of these features providing detailed geomorphic responses of embryos at different life stages of evolution. While variation in the rate of expansion has been observed (i.e. embryos A and B), the expansion and geomorphic response following capture has been largely consistent suggesting a common process oriented evolution that must be studied moving forward.

Incipient blowouts have been described in the literature but prior to this study little were known about the geomorphology of these features. With the aid of TLS, these features can now be studied in great spatial and temporal resolution. Embryos are a form of incipient blowouts and the data presented here furthers our understanding of recently initiated blowouts, but, they are also unique landforms that have significant geomorphic implications. Previous studies documenting the evolution of blowouts haven't accounted for the rapid expansion of blowouts through embryo dune capture. Embryos initiate, expand rapidly, and potentially become capture all within in a sub decadal time scale. Following capture the overall blowout area becomes greatly increased and large amounts of new sediment are introduced into the system. The role of embryo blowouts at Provincelands is unquestionable as they are pervasive on the landscape; however, these features need to be studied at different blowout environments to determine their significance on long term blowout evolution that is universally applicable.

Embryo dune blowouts provide a new consideration on our knowledge on the long term development of dune blowouts through rapid modifications to the landform. This study provides

a detailed geomorphic analysis of embryo dunes; however, the processes that drive these features and their role in other locations remain unknown. It was this research's hypothesis that secondary airflow (i.e. recirculation of flow up and along the lee slope) is responsible for initiation and expansion of embryos but further research must be conducted to verify this assumption. Embryos have been observed at other locations in Cape Cod but the other studies on blowouts have failed to distinguish these features as unique or significant features. If these features are widespread at various locales and they evolve in similar ways that were documented in this study, then their role should be considered in a new model which addresses the evolution of blowouts through embryo dune capture. It is known that at Provincelands dunes, embryo dune blowouts have an indelible role in the long term evolution of both blowouts and the larger dune field.

Chapter 4: Conclusion

Previous studies on the geomorphology of blowouts have been limited due to the lack of emphasis on blowout evolution and limitations in monitoring techniques. The two studies presented in this thesis provide an in-depth geomorphic study that presents a greater understanding of dune blowout geomorphology. This was achieved by conducting both new forms of blowout analysis while also monitoring basic dune blowout evolution (i.e. elevation change and areal expansion). High-resolution geomorphic mapping has allowed for the accurate quantification of blowout geomorphology. Detailed DEMs, generated from TLS point clouds, permits the monitoring of small and large scale changes in elevation change and areal expansion. Previous studies monitored blowout evolution through the use of aerial photos (Jungerius and van der Muelen, 1989), erosion pins (Jungerius and van der Muelen, 1989; Gares, 1992; Pluis, 1991; Gares and Nordstrom, 1995; Hugenholtz and Wolfe, 2006; and Hansen et al. 2009), and tachymetric leveling (Kayhko, 2007). This research methodology goes beyond previous studies by providing detailed coverage across the entirety of the landform surface making limitations in spatial coverage less pronounced. The detailed study of dune blowout evolution increases our understanding of aeolian dune dynamism. The importance of the findings lies in society's ability to take this information and provide a broader understanding of the evolution of blowouts in coastal management.

Large-scale geomorphic changes were observed on both the annual and seasonal scales. During the two annual surveys the study trough blowout experienced greater than 800 m^3 of erosion and the depositional lobes had up to 615 m^3 of deposition. Most topographic changes within blowouts are driven by high magnitude wind events. Storm events generally impact

Provincelands dunes during the fall and winter months and the majority of change to occur during these periods. Depositional lobes appear to accumulate more sediment during high frequency lower magnitude wind events during the summer months. The ability to monitor a blowout in high spatial and temporal resolution has provided a new level of understanding of the sensitivity of blowouts to variations in seasonal and annual temporal scales.

The systematic classification of sub-landforms features within a complex trough blowout has provided new insight to blowout dynamics. Small-scale changes recorded here provide a broader understanding of the geomorphology of blowouts. Areas with increased slope (i.e. scarp, lateral wall, and transport ramp) often experienced the highest levels of erosion, while the areas of decreased slope experienced higher levels of deposition or relative inactivity (i.e. deflation basin and the throat). These results then allow us to have a greater understanding on observations made in the field. For instance during the first year of this study the deflation basin experienced high levels of erosion, but, following the fall and winter season this area was observed to be inundated with water or experiencing increased moisture content suggesting it has eroded down to the high water table. The sediment budget during the second year shows a geomorphic zone (i.e. the deflation basin) as being an area of deposition. The increased moisture content in this area would make aeolian transport increasingly difficult and we are now able to quantify the geomorphic response at the sub-landform scale. The ability to map sub-landform features allows researchers to systematically address small-scale features that are driving larger scale changes at the landform scale.

Topographic steering within trough blowouts can be highlighted by the examination of the Sediment Drift Potential model in comparison to actual sediment drift within the blowouts. Regional wind data is not an ideal method to address on-site sediment drift; however, it can

provide a local context in which storm events (i.e. > 12 m/s) are impacting the study site. Storm events with an incipient angle oblique to the study trough blowout are being topographically steered parallel to the axis because erosion within the blowout maintained an orientation parallel to this axis at all time scales. Although the storm events were occurring from various directions, the erosion within the blowout remained consistent. The study blowout is primarily oriented to northwest winds; however, other high magnitude northerly winds are being topographically steered into the blowout causing accelerated erosion through the primary axis.

Embryo blowouts are a unique form of incipient blowout that has been first described in this study. Embryos form within a few meters in the lee of the crest of elevated blowout and dune ridges. These features expand rapidly upon initiation and can become capture by the host feature in a period of only a few years. The geomorphic significance of these features is their ability to rapidly modify their host blowouts following capture. Rapid modification to blowout landforms due to this process greatly exceeds changes that would be expected at the annual and seasonal scales. As blowouts develop they expand primarily downwind of the crest and laterally. The upwind section becomes encroached upon by the host feature. As the ridge that separates the two landforms narrows, capture of the embryo occurs during high magnitude wind events breach the barrier. After capture embryos introduce large amounts of sediment to be transported to the host feature. The newly exposed opening acts to funnel and accelerate airflow further eroding the once sheltered embryo. The broader importance of these features is that they provide a new model for larger blowout evolution that has not considered the impact of rapid modification due to embryo capture.

A new theoretical model was proposed for the initiation and development of embryo dunes. Only four embryos were documented for this study, however, they are persistent at Provincelands dunes making a model of their development relevant given their greater geomorphic significance on the landscape. The model states that deposition occurs in the lee providing layers of loose unconsolidated sediment. Initiation then occurs in the lee of the crest due to the effects of secondary airflow (i.e. recirculation back-up and along the lee slope). The embryo then expands rapidly and is maintained through these secondary airflow conditions. Embryo capture takes place on a sub-decadal time scale. Finally, after capture rapid expansion and erosion of both the host and former embryo occurs. This model makes a few key assumptions, primarily that the study embryos are representative of the larger population of embryos at the study site and that secondary airflow patterns are responsible for the initiation and expansion of these feature. Process oriented studies can be designed to test these secondary airflow characteristics. For instance, a series of vertical transects upwind and downwind of the crest can monitor airflow over the crest. Simultaneously sensors could be placed along the longitudinal and lateral axis of the embryo to monitor airflow within the embryo. This proposed anemometer experiment could provide a model to capture the effects of secondary airflow within embryos during field experiments. In order to verify this model future research must be conducted to test these assumptions but it was beyond the scope of this initial research.

Future studies on the geomorphology of blowouts will likely expand upon and refine the methodology that was used in the current study. Continual advancements in technology (e.g. remote sensing) will provide better ways in which both landform and landscape evolution can be monitored. Better mapping techniques in both LiDAR and aerial photography will provide more detailed maps that can be used at multiple scales (i.e. landform and landscape). Currently our

TLS data provides excellent detail but only across a relatively small spatial extent. In comparison, the aerial photos collected for the embryo blowout study provided a landscape wide coverage but little detail remained at the landform scale. By providing detailed sediment budgets at both the landform and sub-landform scale a new understanding on blowout development in response to annual and seasonal scales has been gained. Topographic steering within blowouts based on regional wind data has been examined showing the multi-directional storm events cause erosion parallel to the primary axis of the blowout. The identification and monitoring of embryos may provide the largest contribution of this research to the greater blowout literature. Embryos greatly modify the host blowout after capture and provide a new evolutionary track of blowout development. While this study has provided a detailed geomorphic analysis of embryos, future research must test the theoretical model of development by testing the processes that initiate and expand these features. Overall, this study has provided high resolution spatial and temporal resolution data to greatly enhance our knowledge of the geomorphology of blowouts. While this is the first step to better understand the dynamics of dune blowouts, future research must integrate the detailed geomorphic studies with equally detailed process oriented data to enhance our knowledge of blowouts even further.

References

Anderson, J. L. and I.J. Walker, 2006. Airflow and sand transport variations within a backshore-parabolic dune plain complex: NE Graham Island, British Columbia, Canada. Geomorphology 77: 17-34.

Bagnold, R.A. 1941. The Physics of Blown Sand and Desert Dunes, Chapman & Hall.

Bate, G., and M. Ferguson. 1996. Blowouts in coastal foredunes. Landscape and Urban Planning 34: 165-414.

Belly, P.Y. 1964. Sand movement by wind. U.S. Army Coastal Engineering Research Center Technical Memorandum 1:1-38.

Bullard, J.E. 1997. A note on the use of the "Fryberger Method: for evaluating potential sand transport by wind. Journal of Sedimentary Research 67 (3): 499-501.

Davidson-Arnott , R.G.D. and M.N. Law. 1990. Seasonal patterns and controls on sediment supply to coastal foredunes, Long Point, Lake Erie. Coastal Dunes: Processes and Geomorphology, New York: Wiley: 177-200.

Davidson-Arnott, R.G.D., Y. Yang, J. Ollerhead, P.A. Hesp and I.J. Walker. 2007. The effects of surface moisture on aeolian sediment transport threshold and mass flux on a beach. Earth Surf. Process. Landforms 33: 55-74.

Den Van Ancker, J.A.M., P.D. Jungerius and L.R. Mur. 1985. The role of algae in the stabilization of coastal dune blowouts. Earth Surface Processes and Landforms 10: 189-192.

Evans, I.S. 2012. Geomorphometry and landform mapping: What is a landform? Geomorphology 137 (1): 94-106

Forman, S.L., Z. Sagintayev, M. Sultan, S. Smith, R. Becker, M. Kendall and L. Marin. 2008. The twentieth-century migration of parabolic dunes and wetland formation at Cape Cod National Sea Shore, Massachusetts, USA: landscape response to a legacy of environmental disturbance. The Holocene 18 (5): 765-774.

Fraser, G.S., S. W. Bennett, G. A. Olyphant, N. J. Bauch, V. Ferguson, C.A. Gellasch, C. L. Millard, B. Mueller, P. J. O'Malley, J. N. Way and M. C. Woodfield. 1998. Windflow Circulation Patterns in a Coastal Dune Blowout, South Coast of Lake Michigan. J. Coastal Research 14 (2): 451-460.

Fryberger S.G. and G. Dean. 1979. Dune Forms and Wind Regime. A study of Global Sand Seas; Geological Survey Professional Paper 1052: 137-169.

Gares, P.A. 1992. Topographic changes associated with coastal dune blowouts at island beach state park, New Jersey. Earth Surface Processes and Landforms 17 (6): 589-604.

Gares, P. A. and K. F. Nordstrom. 1995; A Cyclic Model of Foredune Blowout Evolution for a Leeward Coast: Island Beach, New Jersey. Annals of the Assoc. Amer. Geographers 85 (1): 1-20.

Hansen, E., S. DeVries-Zimmerman, D. van Dijk and B. Yurk. 2009. Patterns of Wind Flow and Aeolian Deposition on a Parabolic Dune on the Southeastern Shore of Lake Michigan. Geomorphology 105: 147-157.

Hesp, P.A. 1996. Flow Dynamics in a Trough Blowout. Boundary-Layer Meteorology 77: 305-330.

Hesp, P.A. and R. Hyde. 1996. Flow dynamics and geomorphology of a trough blowout. Sedimentology 43 (3): 505-525.

Hesp, P.A. and A. Pringle. 2001. Wind flow and topographic steering within a trough blowout. Journal of Coastal Research (ICS 2000 Proceedings): 597-601.

Hesp, P. 2002. Foredunes and blowouts: initiation, geomorphology and dynamics. Geomorphology 48: 245-268.

Hesp, P. and I. J. Walker. 2012. Three-dimensional aeolian dynamics within a bowl blowout during offshore winds: Greenwich Dunes, Prince Edwards Island, Canada. Aeolian Research 3: 389-399.

Hugenholtz, C.H. and S.A. Wolfe. 2006. Morphodynamics and climate controls of two aeolian blowouts on the norther Great Plains, Canada. Earth Surfaces Processes and Landforms 31 (12): 1540-1557.

Hugenholtz, C.H. and S.A. Wolfe. 2009. Form-flow interactions of an aeolian saucer blowout. Earth Surface Processes and Landforms 34 (7): 919-928.

Jungerius, P. D. and F. van der Muelen. 1989. The Development of Dune Blowouts, As Measured With Erosion Pins and Sequential Air Photos. CATENA 16: 369-376.

Jungerius, P.D., A.J.T. Verheggen and A.J. Wiggers. 1981. The development of blowouts in 'de blink,' a coastal dune area near Noordwijkerhout, The Netherlands. Earth Surface Processes and Landforms 6: 375-396.

Jungerius, P.D., J.V. Witter and J.H. van Boxel. 1991. The effects of changing wind regimes on the development of blowouts in the coastal dunes of the Netherlands. Landscape Ecology 6:41-48.

Kayhko, J. 2007.Aeolian Blowout Dynamics in Subarctic Lapland Based on Decadal Levelling Investigations. Geografiska Annaler: Series A, Physical Geography 89 (1): 65-81.

Neal, A., and C.L. Roberts. 2001. Internal structure of a trough blowout, determined from migrated ground-penetrating radar profiles. Sedimentology 48: 791-810

Pearce, K.I. and I.J. Walker. 2005. Frequency and magnitude biases in the 'Fryberger' model, with implications for characterizing geomorphically effective winds. Geomorphology 68 (1-2): 39-55.

Pluis J. L. A. 1992. Relationships Between Deflation and Near Surface Wind Velocity in a Coastal Dune Blowout. Earth Surface Processes and Landforms 17: 663-673

Smith, H.T.U. 1960. Physiography and photo interpretation of coastal sand dunes. Final Report Contract NONR-2242(00), Office of Naval Research, Geographical Branch, 60 pp.

Smith, A.B. 2013. Geomorphology of Dune Blowouts, Cape Cod National Seashore, MA. M.A. Thesis: 1-90.

Smith, S.M., R.M.M Abed and F. Garcia-Pichel. 2004. Biological Soil Crusts of Sand Dunes in Cape Cod National Seashore, Massachusetts, USA. Microbial Ecology 48: 200-208.

Smyth, T.A.G., D.W.T. Jackson and J.A.G. Cooper. High resolution measured and modeled three-dimensional airflow over a coastal bowl blowout. Geomorphology 177-178: 62-73.

Staley, D., Wasklewicz, T., Coe, J., Kean, J., McCoy, S., and Tucker, G.E. (2011). Observations of debris flows at Chalk Cliffs, Colorado, USA: Part 2, changes in surface morphometry from terrestrial laser scanning in the summer of 2009. In Genevois, R., Hamilton, D.L., and Prestininzi, A (Eds.), Proceedings of the 5th International Conference on Debris Flow Hazards Mitigation, Mechanics, Prediction and Assessment, Padua, Italy, Rome, Italy: Italian Journal of Engineering Geology and Environment and Casa Editrice Universita La Sapienza, p. 759-768.

Staley, D., Wasklewicz, T., and Kean, J. (under review). Characterizing the primary material sources and dominant erosional processes for a post-fire debris flow event using multi-temporal terrestrial laser scanning data. *Geomorphology*.

Von Karman, T., and C.B. Millikan. 1934. On the Theory of Laminar Boundary Layers Involving Seperation. National Advisory Committee for Aeronautics: 541-560.

Zingg, A.W. 1954. The wind erosion problem in the Great Plains. American Geophysical Union 35: 252-258